MODIFICATIONS OF CORTICAL ACTIVITY BY DEEP BRAIN STIMULATION IN ADVANCED PARKINSON'S DISEASE: AN MEG STUDY

Katja Airaksinen

Department of Neurology

BioMag Laboratory
HUS Medical Imaging Center

Helsinki University Hospital

Faculty of Medicine
Doctoral Programme in Brain & Mind
University of Helsinki

ACADEMIC DISSERTATION

To be publicly discussed
with the permission of
the Medical Faculty of the University of Helsinki
in lecture hall 1, Meilahti Hospital
on November 6, 2015, at 12 noon

Helsinki 2015

SUPERVISORS Docent Eero Pekkonen
Department of Neurology
University of Helsinki and Helsinki University Hospital
Finland

Docent Jyrki P. Mäkelä
BioMag Laboratory
HUS Medical Imaging Center
University of Helsinki and Helsinki University Hospital
Finland

REVIEWERS Docent Valtteri Kaasinen
Department of Neurology
Turku University Hospital
Finland

Professor Esa Mervaala
Department of Clinical Neurophysiology
Kuopio University Hospital
Finland

OPPONENT Clinical Professor Karen Østergaard
Department of Neurology
Aarhus University Hospital
Denmark

Published in series *Dissertationes Scholae Doctoralis Ad Sanitatem Investigadam Universitatis Helsinkiensis*

ISBN 978-951-51-1609-3 (paperback)
ISSN 2342-3161 (print)
ISBN 978-951-51-1610-9 (PDF)
ISSN 2342-317X (online)

http://ethesis.helsinki.fi

TABLE OF CONTENTS

LIST OF ORIGINAL PUBLICATIONS

This thesis is based on the following original publications that will hereafter be referred to in the text by their Roman numerals (I – IV).

I. **Effects of DBS on auditory and somatosensory processing in Parkinson's disease**

   Airaksinen K, Mäkelä JP, Taulu S, Ahonen A, Nurminen J, Schnitzler A and Pekkonen E.

   Human Brain Mapping 2011;32:1091–1099

II. **Somatomotor mu rhythm amplitude correlates with rigidity during deep brain stimulation in Parkinsonian patients**

   Airaksinen K, Butorina A, Pekkonen E, Nurminen J, Taulu S, Ahonen A, Schnitzler A and Mäkelä JP.

   Clinical Neurophysiology 2012;123:2010–2017

III. **Cortico-muscular coherence in advanced Parkinson's disease with deep brain stimulation**

   Airaksinen K, Mäkelä JP, Nurminen J, Luoma J, Taulu S, Ahonen A and Pekkonen E.

   Clinical Neurophysiology 2015;126:748–755

IV. **Cortico-muscular coherence parallels coherence of postural tremor and MEG during static muscle contraction**

   Airaksinen K, Lehti T, Nurminen J, Luoma J, Helle L, Taulu S, Pekkonen E and Mäkelä JP.

   Neuroscience Letters 2015;602:22–26

The thesis also contains some unpublished data, which is referred to as additional material.

ABBREVIATIONS

6-OHDA	6-hydroxydopamine
AEF	Auditory evoked fields
BG	Basal ganglia
CKC	Corticokinematic coherence
CMC	Cortico-muscular coherence
COMT	Catechol-O-methyltransferase
DBS	Deep brain stimulation
DFT	Discrete Fourier transform
DICS	Dynamic imaging of coherent sources
ECD	Equivalent current dipole
EcoG	Electrocorticography
EEG	Electroencephalography
EMG	Electromyography
EOG	Electrooculography
F	Female
FFT	Fast Fourier transform
fMRI	Functional magnetic resonance imaging
GABA	Gamma-amino butyrate
GP	Globus pallidus
GPe	Globus pallidus external
GPi	Globus pallidus internal
ICH	Intra cerebral haemorrhage
ISI	Interstimulus interval
LCIG	Levodopa-carbidopa intestinal gel
LEDD	Levodopa equivalent daily dose
LFP	Local field potential
M	Male
M1	Primary motor cortex
MAO	Monoamine oxidase
MCE	Minimum current estimate
MCEfd	Frequency domain minimum current estimate
MEG	Magnetoencephalography
MNE	Minimum norm estimate
MRI	Magnetic resonance imaging
MU	Motor unit
n	Number
N	Vertex negative

PCB	polychlorinated biphenyl
PD	Parkinson’s disease
PET	Positron emission tomography
PIGD	Postural instability gait disorder
PPN	Pendunculopontine nucleus
PSD	Power spectral density
ROI	Region of interest
SI	Primary somatosensory cortex
SII	Secondary somatosensory cortex
SEF	Sensory evoked field
SEP	Sensory evoked potential
SN	Substantia nigra
SNpc	Substantia nigra pars compacta
SNpr	Substantia nigra pars reticulata
SPECT	Single-photon emission computed tomography
SQUID	Superconducting quantum interference device
SSS	Signal Space Separation
STN	Subthalamic nucleus
tACS	Transcranial alternating current stimulation
TMS	Transcranial magnetic stimulation
tSSS	Spatiotemporal signal space separation
UPDRS	Unified Parkinson's rating scale
Vim	Ventral intermediate nucleus

ABSTRACT

Aims: The aims of this PhD research were to study the feasibility of magnetoencephalography (MEG) measurements in Parkinson's disease (PD) patients treated with deep brain stimulation (DBS) of subthalamic nucleus (STN) and to cast light onto the effects of DBS on the electrical activity of the brain. The ultimate aim was to gain a better understanding of the unclear therapeutic mechanism of DBS.

MEG is very sensitive to magnetic fields and it is used as a powerful tool to study noninvasively the brain's electromagnetic activity with an excellent time resolution and reasonable spatial resolution. The sensitivity, however, makes the measurements of patients using electrical devices challenging because of confounding artifacts that partly or completely obscure the measured signals. An artifact suppression method called spatiotemporal signal space separation (tSSS) was developed shortly before the beginning of this thesis project. One aim was to investigate how tSSS works in the suppression of DBS artifacts in patients undergoing DBS treatment. We also used MEG to study the effects of DBS on spontaneous brain rhythms and on cortico-muscular coherence (CMC) in PD patients. An accelerometer device detects the three-dimensional acceleration during movements, including tremor. We used this tool to study healthy volunteers to understand better the nature of CMC.

Methods: These studies were performed with a 306-channel MEG device in the BioMag Laboratory in Helsinki University Hospital. The measured MEG signals included evoked responses, spontaneous brain activity and CMC in advanced PD patients that were being treated with DBS. A total of 24 PD patients were included in the studies. CMC and corticokinematic coherence (CKC) were also studied in 10 healthy subjects. The effect of DBS was measured with DBS first being on and then turned off as a crossover treatment. The patients thus served as their own controls for the two conditions. Antiparkinsonian medication was continued throughout the measurements. The Unified Parkinson's rating scale (UPDRS)-III functional test was performed with DBS on and off to correlate the MEG results with the clinical condition.

Somatosensory evoked fields (SEFs) were elicited by electrical 200-μs square-wave pulses that were delivered to the median nerve. Auditory evoked fields (AEFs) were elicited by 1-kHz sinusoidal 50-ms tones. Spontaneous brain oscillations were recorded with the eyes closed and open. For CMC recordings, MEG was recorded simultaneously with surface EMG over the activated extensor carpi radialis muscle. The healthy volunteers had an accelerometer sensor attached to their index fingernail for the CKC measurements. The motor task was to hold dorsiflexion of the wrist five times for one minute. Most patients and all volunteers had brain MR images to combine with the MEG results. tSSS was used for artifact suppression.

Results: tSSS reduced the DBS artifacts. This reduction enabled reliable MEG signal analysis for most patients. Some residual artifacts remained even after tSSS. Hence, the careful scrutiny of data was important even after tSSS.

The effects of DBS on the brain's electrical activity varied considerably between patients. However, several statistically significant group effects were observed. AEF N100m amplitude increased in the right hemisphere for ipsilateral stimulation during DBS. When the DBS was on, the mu rhythm amplitude of spontaneous MEG correlated significantly with the UPDRS rigidity measures. The CMC was detected in 15 out of 19 PD patients, as described previously in healthy control subjects. We did not find a systematic increase in CMC in the 13 – 25 Hz band during DBS.

CKC could be recorded during the static wrist extension task in healthy subjects. The source locations of CMC and CKC were overlapping and their spectral profiles resembled each other.

Conclusions: tSSS is extremely useful in the artifact suppression of MEG measurements of DBS patients. Despite this, MEG measurements of DBS patients are still challenging and need exact planning of the experimental setups and caution in the data analysis. DBS modifies cortical electrical activity, and some of these modifications correlate with the clinical improvement in PD. The accelerometer device accurately detects even small movements during a hold task and may turn out to be a good alternative to EMG for coherence calculations.

1. INTRODUCTION

Parkinson's disease (PD) is a common progressive neurodegenerative disease with clinical symptoms of bradykinesia, rigidity and resting tremor. It is caused by a gradual destruction of the dopaminergic cells in the substantia nigra. The brain oscillations have an important role in the pathophysiology of PD. The disease is characterized by abnormally synchronized beta band activity in the subthalamic nucleus (STN) and the globus pallidus internal (GPi) (Bronte-Stewart et al., 2009).

Levodopa has remained the most effective drug to relieve the motor symptoms of PD. Long lasting use of high-dose levodopa probably gives rise to daily motor fluctuations that can be delayed by using dopamine agonists and /or monoamine oxidase (MAO)-B inhibitors. However, long-term levodopa treatment eventually gives rise to unfavorable effects. The most common symptoms are daily motor fluctuations such as “wearing off” (the appearance of PD symptoms before the next levodopa dose) or on-off phenomenon (phases of mobility alternating with immobility) and dyskinesias. When severe drug resistant motor fluctuations and dyskinesias appear, three treatments are available: 1) deep brain stimulation (DBS), 2) levodopa-carbidopa intestinal gel (LCIG) infusion or 3) apomorphine pump. DBS is a well documented treatment in advanced PD (Krack et al., 2003; Deuschl et al., 2006; Weaver et al., 2009; Schuepbach et al., 2013). Although DBS is an established treatment for advanced PD, its precise mechanism of action is still unclear (McIntyre et al., 2004; Montgomery Jr and Gale, 2008; Miocinovic et al., 2013).

The study of DBS action mechanisms in patients is challenging. All the major functional brain imaging modalities have some limitations in studying the effects of DBS treatments. Functional magnetic resonance imaging (fMRI) and positron emission tomography (PET) imaging are based on the changes in blood flow or circulation-distributed ligand binding but measures of these parameters result in poor time resolution in respect of brain oscillations. Haemodynamic measurements are also an indirect estimation of neural activation. Moreover, the magnetic fields generated in fMRI are an obvious risk to DBS patients. The magnetic fields may damage or overheat the DBS device. PET and DBS devices do

not interfere with each other but PET measurements require the use of ionizing radiation. This limits the serial measurements by such a method.

Electroencephalography (EEG) and magnetoencephalography (MEG) are direct measurements of neural activity and are also safe for DBS patients. The problems with these methods are associated with the electromagnetic artifacts produced by DBS. A novel artifact suppression method, spatiotemporal signal space separation (tSSS) (Taulu and Simola, 2006), makes it possible to analyze MEG data that are contaminated by DBS artifacts. When such artifact problems are solved, MEG is a useful non-invasive tool for the study of the electromagnetic activity of the brain in excellent time and good spatial resolution also in DBS patients.

The studies that are summarised in this thesis investigated the feasibility of tSSS in analyzing and evaluating DBS-treated PD patients measured by MEG. The aim was to investigate the effect of DBS on the electromagnetic activity of the brain. The evoked fields, spontaneous brain activity and cortico-muscular coherence (CMC) of STN-DBS treated Parkinsonian patients were measured. One study in healthy subjects that utilized corticokinematic coherence (CKC) in addition to CMC was also carried out to interpret better the results of CMC.

2. REVIEW OF THE LITERATURE

2.1 Parkinson's disease

2.1.1 Epidemiology of PD

Parkinson's disease is a neurodegenerative disorder that is caused by the destruction of dopaminergic cells in the substantia nigra. It is the second most common neurodegenerative disease after Alzheimer's disease and the second most common movement disorder after essential tremor. PD occurs predominantly in the elderly. Only 4% of PD patients get the symptoms before the age of 50 years (Alves et al., 2008). The prevalence of PD is about 0.5% for the 60 – 69 years cohort, and it increases up to 2% in people older than 80 years (Pringsheim et al., 2014) or even up to 4% (de Lau and Breteler, 2006). The age-adjusted prevalence of PD in the beginning of 1990s in Finland was 166 per 100 000 population (Kuopio et al., 1999). The incidence of PD increases as the population gets older. This is especially the case in males as the male-to-female incidence rate ratio increases (Kaasinen et al., 2015). There are approximately 15 000 PD patients in Finland.

The aetiology of PD is unclear in most cases. Cigarette smoking and coffee consumption are lifestyle factors that are consistently associated with a reduced risk of PD. Other factors that have also been associated with reduced risk of PD are exercise, the use of non-steroidal anti-inflammatory medications, and use of dihydropyridine calcium channel-blocking drugs (Goldman, 2014). Exposure to pesticides, particularly to polychlorinated biphenyls (PCBs) is a possible risk factor for PD (Goldman, 2014). Mutations in seven genes are associated with either autosomal dominant or recessive forms of PD or parkinsonism. PD or parkinsonism are also suggested to be caused by changes in many additional genes related e.g. to frontotemporal dementia or hereditary ataxia. The known genetic mutations are very rare in most populations, and thus explain probably fewer than 5% of all PD cases. (Puschmann, 2013)

2.1.2 Symptoms and disease progression in PD

Resting tremor (shaking), bradykinesia (slowness of movements) and rigidity (stiffness, increase in muscle tone) are the well-known triad of motor symptoms in PD. Postural instability and falls are common in advanced PD. In addition to motor symptoms, PD patients also suffer from non-motor symptoms such as hyposmia, problems in the autonomic nervous system (causing e.g. postural hypotension and constipation), sleep disturbances, depression and dementia (Seppi et al., 2011). Some of the non-motor symptoms may precede the motor symptoms and diagnosis by several years.

The progression rate of PD varies considerably between different patients. In an individual patient, the motor symptoms progress quite constantly. The tremor-dominant type of disease is thought to have a more favourable prognosis than the hypokinetic variant (Marttila et al., 1991; Eggers et al., 2012). Higher postural instability gait disorder (PIGD) score at baseline is related to an increased mortality hazard ratio when adjusted for age, sex and disease duration (de Lau et al., 2014) and also to more rapid cognitive decline (Burn et al., 2006). PD increases mortality; the standardized mortality ratio has been reported to range from 0.9 to 3.8; inception cohorts showed a pooled mortality ratio of about 1.5 (Macleod et al., 2014). However, about 10 % of patients have a benign course (Hely et al., 1999). PD patients with dementia have an increased risk of mortality compared with PD patients without dementia (Hobson et al., 2010; Willis et al., 2012). Patients who do not develop dementia appear to have near normal population mortalities (Hobson et al., 2010). Baseline characteristics including the male gender, older age at diagnosis, higher baseline Hoehn & Yahr stage, higher baseline UPDRS motor scores, higher bradykinesia subscores and cognitive impairment were all reported to be related to early mortality in PD (Oosterveld et al., 2015).

2.1.3 Physiology and pathophysiology of the basal ganglia in PD

The basal ganglia (BG), consist of the striatum, the globus pallidus (GP), the substantia nigra (SN) (consisting of the pars pars reticulata and pars compacta) and STN, are affected in PD (DeLong, 2000). The hallmark of PD is the progressive loss of dopaminergic neurons in the SN pars compacta and cytoplasmic inclusions (Lewy Bodies). The α-synuclein

protein is the principal component of Lewy Bodies. The α-synuclein might be a prion-like protein, being capable to adopt a self-propagating conformation and causing neurodegeneration (Olanow and Brundin, 2013). Early neuropathological findings suggest that about 60% of the dopaminergic neurons in the SN pars compacta will already have been lost at the onset of motor PD symptoms (Schulz and Falkenburger, 2004).

The putamen is the most important afferent structure of the basal ganglia. Two separate pathways originate from the putamen. One of them, the direct pathway, inhibits the GPi and the other, the indirect pathway, inhibits the globus pallidus external (GPe) which in turn inhibits the STN. An excitatory projection connects the STN to the GPi. Inhibitory gamma-aminobutyrate (GABA)-ergic projections from the GPi suppress thalamic neural activity. The thalamocortical excitatory projections extend to the cortex.

Decreased dopamine action impairs the direct pathway from the putamen to the GPi whereas the projection via the indirect pathway to the GPe is overactive. These events lead to the disinhibition of GPi and to the increased inhibition of the thalamocortical neurons. This is called the classic pathophysiological model (Figure 1) of PD (Albin et al., 1989; DeLong, 1990; Delwaide et al., 2000).

Some data support the idea that the STN is another input station for the BG. The hyperdirect pathway (Figure 1) projects from the cortex directly to the STN. It bypasses the striatum, and goes further to the GPi. The hyperdirect pathway is activated by the initiation of voluntary movement, which leads to inhibition of large areas of the thalamus and the cerebral cortex. Soon after, the signal from the direct pathway disinhibits these targets and only the selected ‘motor program’ is run. Eventually, the indirect pathway inhibits the targets thoroughly (Nambu et al., 2002).

It is also possible that other output recipients for the BG exist apart from the cortex. BG may also project into the tegmentum, including pedunculopontine nucleus (PPN). Signaling in this pathway probably prepares the spinal cord neurons for cortical motor commands (Delwaide et al., 2000).

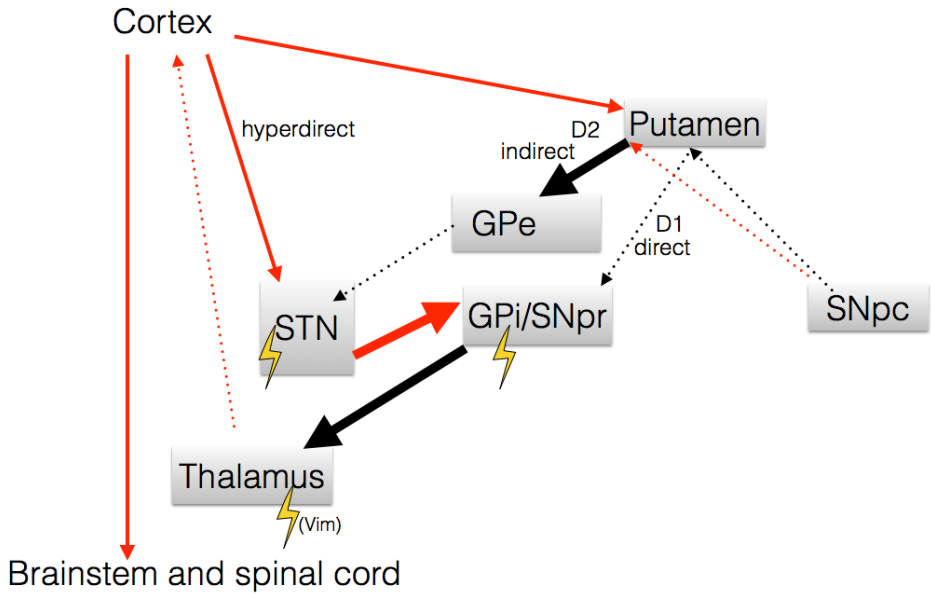

Figure 1. A simplified scheme of the basal ganglia-thalamo-cortical circuit. The black arrows indicate inhibitory and the red arrows excitatory connections. The dotted arrows represent weaker connections and the bold arrows stronger connections in PD than in healthy subjects. Cell loss in the substantia nigra pars compacta (SNpc) leads to an overactivation of the indirect, dopamine D2-receptor mediated movement-suppressing pathway and an inhibition of the direct D1-receptor mediated movement facilitating pathway. This leads to inhibition of the thalamus. The DBS sites that are targeted most often in PD treatment are marked with a flash sign.
GPe= globus pallidus external, GPi= globus pallidus internal, SNpc= substantia nigra pars compacta, SNpr= substantia nigra pars reticulata, STN=subthalamic nucleus, Vim=ventral intermediate nucleus

Untreated PD patients have been characterized to have abnormally synchronized beta band (13 – 35 Hz) activity in the STN and the GPi (Brown et al., 2001; Priori et al., 2004; Bronte-Stewart et al., 2009). Coherence between the local field potentials (LFPs) that emanate from STN and cortical sensorimotor oscillatory activity measured by MEG has been reported (Litvak et al., 2010, 2012; Hirschmann et al., 2011). Beta band oscillatory activity in the STN is decreased prior to movement and increases during voluntary suppression of movements (Kühn et al., 2004). Improvement of akinesia and rigidity, contrary to tremor, are associated with reduction in STN 8 – 35 Hz activity (Kühn et al., 2006). STN 15-Hz

oscillations have a tendency to correlate with the amelioration of rigidity by medication, whereas oscillations around 25-Hz are associated with an improvement in axial bradykinesia by DBS (Zaidel et al., 2010). Activity and firing rate of STN neurons may increase with the progression of PD (Remple et al., 2011). The beta band may be functionally divided. The lower beta band (<20 Hz) might be more suppressed by dopaminergic medication than the upper beta band (Priori et al., 2004). STN activity may correlate in this lower beta band with the oscillatory activity in the sensorimotor cortex (Fogelson et al., 2006). Moreover, worsening of PD patient's motor symptoms is achieved by the stimulation of the STN at 10 H z (Timmermann et al., 2004), or in the 5 –10 Hz or 20 – 25 Hz frequency bands (Fogelson et al., 2005).

2.1.4 Treatment

Currently, all treatment options relieve PD symptoms. No established treatment to cure or stop the disease progression exists so far. The medical treatment of PD is based on increasing dopaminergic activity in the brain. Three main groups of medication are levodopa, dopamine agonists and MAO-B inhibitors.

Levodopa was introduced in the late 1960s, and it is the most effective medication for PD patients (Carlsson, 2002). Levodopa is the precursor of the neurotransmitters dopamine, adrenaline and noradrenaline. Dopamine per se does not cross the blood brain barrier as easily as levodopa does. Aromatic L-amino acid decarboxylase, also known as DOPA decarboxylase, converts levodopa to dopamine in the central and peripheral nervous systems. Levodopa preparations include a peripheral DOPA decarboxylase inhibitor or cathecol-O-methyloxidase (COMT) inhibitors as adjuvants, which inhibit the conversion of levodopa to dopamine before it crosses the blood brain barrier. The aim is to increase dopamine concentration in the central nervous system while reducing the side effects caused by the action of peripheral dopamine. Because levodopa has a short half-life, it must be administered several times per day particularly in advanced PD, where the dopamine storage ability of the cells is decreased. After prolonged treatment with levodopa (about 5 – 7 years), severe side effects of the treatment become increasingly common. The predictability of the treatment efficacy disappears; apart from the wearing off-phase, the patient may have sudden off-phases.

Severe dyskinesias may also occur with increasing frequency and duration (Ferreira et al., 2013; Connolly and Lang, 2014). Infusion of LCIG into the duodenum by duodenogastrostomy is used to circumvent these problems (Olanow et al., 2014). The fluctuations in the levodopa concentration, erratic absorption due to dosage, and problems related to stomach emptying and nutrition are less severe with LCIG treatment.

Dopamine agonists are also important in the treatment of PD. Agonists activate the receptors in a similar way as their physiological ligands even in the absence of dopamine. The dose is taken once a day as a tablet (ropinirole and pramipexole) or as a transdermal patch (rotigotine). Dopamine agonists may postpone the appearance of motor fluctuations. Dopamine agonists may cause side effects, especially in elderly patients, who may get confused and experience hallucinations. They may also cause impulsive control disorders, such as gambling, and hyper-sexuality (Perez-Lloret, 2012).

Apomorphine is the most potent, fast acting dopamine agonist. It has a short half-life. Because of almost complete first-pass hepatic metabolism, apomorphine is administered by subcutaneous injection (rescue dose) or as a continuous infusion. Rescue injections for severe off-phase help rapidly (3 – 30 min) and the effect may last for 20 – 120 minutes. An apomorphine pump may be used in PD patients, who still have a good response to levodopa and have frequent off-phases despite optimal peroral drug therapy or use several apomorphine injections per day (Boyle and Ondo, 2015). Currently, the apomorphine pump is not available in Finland (2015).

MAO-B inhibitors (selegiline and rasagiline) primarily reduce the breakdown of dopamine and phenethylamine. The clinical effects of these drugs are modest. They are often used at the onset of the disease, or in the later phase when motor fluctuations occur. The MAO-B treatment needs a concomitant endogenous or exogenous source of dopamine to be effective. Amantadine, an antiviral agent, can be used to alleviate levodopa-induced dyskinesias. Anticholinergic drugs are used rather infrequently nowadays, because of cognitive side effects. (Ferreira et al., 2013; Connolly and Lang, 2014)

The sequence of introduction of these medications for patients usually starts with MAO-B inhibitors and/or dopamine agonists and then

proceeds to levodopa, particularly in young patients. This is done to delay the problems associated with long-term levodopa treatment.

2.1.4.1 Surgery

2.1.4.1.1 Lesional surgery

Ablative surgery has been used as early as 1912 for the treatment of PD. Leriche experimented with bilateral posterior cervical rhizotomy to relieve parkinsonian symptoms (Hariz et al., 2010). The first surgical treatments attempted to diminish tremor by reducing the motor function by resections of the premotor or motor cortex, or by pyramidotomy and pedunculotomy. With these procedures tremor might have been alleviated but at the cost of motor functions, and other PD symptoms such as rigidity were not reduced (Schiefer et al., 2011). The introduction of stereotactic surgery (Spiegel et al., 1947) helped the progress of targeting deep brain structures. Their importance was noticed by chance in 1952 when pedunculotomy was discontinued because of severe bleeding. The artery was ligated, which resulted in an infarction of the medial GP and an improvement of the patient's PD symptoms (Schiefer et al., 2011). Electronic stimulation was also used in 1950s for verifying the target prior to making lesions to treat psychiatric diseases (Hariz et al., 2010). For example, the number of thalamotomies to treat PD in Helsinki University Hospital was over one hundred per year in 1963-1966 and over 80 in 1967 and 1968, but the introduction of oral levodopa treatment quickly decreased surgical treatment for PD (Laitinen, 1972).

2.1.4.1.2 DBS theraphy

The modern era of DBS therapy began in 1987 when Alim-Louis Benabid and his team reported the efficacy of stimulation of the ventral intermediate nucleus (Vim) of the thalamus for PD (Benabid et al., 1987). The same team introduced the chronic stimulation of the STN to treat PD (Limousin et al., 1995). The GPi was also tested as a promising DBS target in mid 1990s based on previously reported efficacy of GPi lesions on symptoms of PD (Siegfried and Lippitz, 1994). The DBS treatment has

surpassed surgical lesion therapies as it is highly effective, reversible and safe. DBS surgery is performed in two phases. First, the intracerebral electrodes are implanted. Second, a subcutaneous generator and wires are implanted in the surface of the chest but only when the stimulation response turns out to be useful (Figure 2).

Figure 2. DBS device (with permission of Medtronic Inc.).

The most common present DBS targets for PD treatment are the STN, GPi, Vim and PPN. Stimulation of the STN ameliorates several PD symptoms and usually enables the reduction of dopaminergic medication. Patients with advanced PD had quite similar improvement in motor symptoms when STN and GPi stimulation were compared, but the possibility for postoperative reduction of dopaminergic medication is less likely for GPi stimulation (Follett et al., 2010). The GPi is also a target for treating primary and some secondary types of dystonia. Vim stimulation can be used in the treatment of PD when tremor is the main symptom, but it does not improve other PD symptoms such as bradykinesia. Vim DBS is also used to treat essential tremor. The PPN is an interesting target for DBS for the treatment of axial symptoms and postural instability but the treatment results are still conflicting (Follett and Torres-Russotto, 2012). The PPN stimulators have not been implanted in PD patients in Finland so far.

The DBS of STN is an established treatment for advanced PD when motor fluctuations and dyskinesias are present despite optimal medical treatment (Krack et al., 2003; Deuschl et al., 2006; Weaver et al., 2009). DBS treatment was reported to be superior to optimal medication also in patients with early motor complications (Schuepbach et al., 2013).

Originally it was supposed that high frequency stimulation inhibits the target as similar effects were seen with ablative surgery. Nowadays, this model is considered to be too simplistic. It may be that instead of 'turning down' the STN activity, DBS treatment actually changes the neural activity pattern of the STN (Garcia et al., 2003). High frequency DBS may suppress the spontaneous activity in STN and generate a new activity pattern in the gamma band (Garcia et al., 2005).

Studying the LFPs of STN during STN-DBS has been demanding because of electrical artifacts induced by the stimulation. Nevertheless, suppressed subthalamic beta oscillations during STN-DBS have been reported by some studies (Giannicola, 2010; Eusebio, 2011; Eusebio et al., 2012). Stationary LFP beta oscillations during DBS have also been reported (Rossi et al., 2008). STN-DBS probably decreases the excessive beta activity in the STN and this may, at least in part, induce the reduction of motor symptoms (Eusebio et al., 2012).

The effect of DBS may differ between neuronal soma and axon, as axons appear to be more sensitive to DBS (McIntyre and Grill, 1999). The minimum time needed to excite a neural element using half of the intensity that causes a threshold response (chronaxie) is around 30 – 200 μs for myelinated axons and about 1 – 10 ms for cell bodies and dendrites. Thus, DBS activates efferent axons more easily than cell bodies (Kringelbach et al., 2007). The strength-duration measurements in patients with GPi or Vim stimulators suggest that the primary targets of stimulation in both nuclei are large myelinated axons (Holsheimer et al., 2000).

Studies that used rodent models of PD indicate that the cortex may play an important role in the effect of DBS. Optogenetic inhibition or excitation restricted to STN neurons was not as effective as direct motor cortical stimulation in reducing Parkinsonian symptoms in mice with 6-OHDA lesions (Gradinaru et al., 2009). Stochastic antidromic spikes that emanate from STN during its stimulation in Parkinsonian rats alter the firing rate of corticofugal projection neurons. This desynchronizes the

excessive cortical beta band oscillatory activity and reduces the symptoms (Li et al., 2012).

The optimal electrode contacts need to be selected for maximum treatment efficacy. Stimulation parameters for DBS include amplitude (voltage / current), frequency and pulse width. The effective voltage ranges usually between 1 – 4 V. Stimulation for efficacious PD treatment requires a relatively high frequency; usually 130 Hz or higher frequencies are required. Lower frequencies, e.g. 60 Hz, may be sometimes beneficial for ameliorating gait symptoms (Moreau et al., 2008). The stimulation mode is usually monopolar but bipolar or combination of two adjacent monopolar contacts can be applied. Moreover, an interleave setting can be used. It is recommended that DBS would be programmed several times during the first 6-month interval after the implantation (Bronstein et al., 2011). Adjustments to stimulation and also switching stimulation 'on' and 'off' are done non-invasively by a programmer device.

Tremor and rigidity may return within minutes after DBS has been switched off in most patients. The entire therapeutic effect of DBS mainly disappears within three hours after switching the stimulator off. After turning the DBS off, the UPDRS motor scores increase to about 75% in 15 – 30 minutes whereas tremor subscores increase within 5 minutes. Axial symptoms return slowly, within two hours after switching off the DBS. (Temperli et al., 2003)

Symptomatic intracerebral haemorrhage (ICH) rates in functional neurosurgery vary between 0 – 9% reported in patient series between years 2001 – 2010; the overall incidence was about 2% (Zrinzo et al., 2012). The rate of atraumatic device-related infection during the first year after implantation was reported to be around 2% (Fenoy and Simpson, 2012). Clearly higher infection rates, of 10%, have also been reported (Weaver et al., 2009). Transient postoperative delirium may be quite common, occurring in 24% of the patients after the DBS operation (Krack et al., 2003). Epileptic seizures have been reported soon after the operation (Østergaard et al., 2002). During a six-month follow-up patients with implanted DBS had more falls, gait disturbances, depression and dystonia compared with the best medical therapy group (Weaver et al., 2009). Weight increase, eyelid apraxia, dysarthria and dementia have been reported with a permanent DBS treatment (Østergaard et al., 2002; Krack et al., 2003).

Indications for the DBS therapy include an advanced idiopathic PD that is still responsive to levodopa. The patients with daily on-off fluctuations, dyskinesias and intolerance to high doses of drugs required for symptom control are good candidates for DBS. The drug-resistant tremor is also suitable for DBS. The age of the patient should generally be below 70 years. It is also important that the patient has realistic expectations of the treatment outcome. DBS will not cure nor stop the disease progression.

Contraindications for DBS treatment include clear dementia, general operation contraindications (such as increased risk of bleeding or anticoagulant treatment that can not be discontinued during the operation), and devices such as defibrillators that could interfere with delivered electrical pulses (Benabid et al., 2009). A slight cognitive decline is acceptable for DBS candidates. Severe drug-resistant psychiatric diseases (depression, psychosis) are also a contraindication for DBS, but receded drug-induced hallucinations are not. Patients with predominantly levodopa-resistant axial symptoms do not benefit from DBS.

Screening of advanced PD patients for DBS in Helsinki University Hospital includes a levodopa challenge test, neuropsychological test, brain MRI and psychiatric assessment when necessary. The preoperative levodopa challenge test is done to verify the levodopa response; >30% reduction in UPDRS III score is regarded as a positive response. Good efficacy of levodopa is also indicative of a good response to DBS (Kleiner-Fisman et al., 2006).

Accepted indications for DBS in Europe are PD, essential tremor, dystonia, epilepsy and obsessive compulsive disorder. Medically refractory epilepsy has been treated with the bilateral stimulation of the anterior nucleus of the thalamus (Fisher et al., 2010). Refractory obsessive compulsive syndromes have previously been treated with anterior capsulotomy; DBS targeting the anterior internal capsule (Abelson et al., 2005) and nucleus accumbens (Sturm et al., 2003) has been used as well.

DBS electrodes have been implanted into the periventricular grey or in the sensory thalamus to treat several types of chronic pain (Levy et al., 1987) as off-label treatment. The best long-term results have been obtained for the treatment of chronic low-back and leg pain and in neuropathic pain of peripheral origin (Rasche et al., 2006). Other

indications of DBS under research include e.g. Tourette's syndrome, cluster headache, depression (Kringelbach et al., 2007) and Alzheimer's disease (Laxton et al., 2010).

2.2 MEG

Magnetoencephalography is used to record weak magnetic fields that are produced by the brain's electrical activity when tens of thousands of nearby neurons act synchronously. Neuromagnetic signals typically occur over the 50 – 500 fT (about 10 – 100fT/cm) amplitude range. For comparison, the steady geomagnetic field of the earth is about one billion (10^9) times stronger. (Hämäläinen et al., 1993)

Advantages of using MEG include complete noninvasiveness, an excellent time resolution, in the range of milliseconds, and a good spatial resolution. The spatial resolution can be a few millimeters at its best. The spatial resolution achieved by MEG is better than that of EEG as the magnetic fields are not distorted by the skull, skull breaches or by other tissues, whereas electrical potentials are sensitive to such confounding factors. Both spontaneous and evoked brain activity can be studied by using MEG. The functional MEG data can also be combined with anatomical information obtained by magnetic resonance imaging (MRI). (Hämäläinen et al., 1993)

2.2.1 Neuronal basis

Activated neurons generate electrical currents and all electrical currents create a magnetic field around them. The intracellular postsynaptic currents in the apical dendrites of cortical pyramidal cells are the main origin of the measured magnetic signals that emanate from the brain (Hari, 1991). Postsynaptic potentials last longer than action potentials. Apical dendrites of pyramidal neurons are oriented in parallel. Both these facts enhance the summation of the magnetic fields (Hari et al., 2010). Action potentials contribute to MEG signals only weakly as their associated magnetic fields attenuate more rapidly than those of the postsynaptic potentials as function of the distance. Moreover, action

potentials of different cells are unlikely to synchronize (Lopes da Silva, 2010).

The dipole moments of a typical evoked magnetic field measured outside the skull are in the order of 10 nAm (Hämäläinen et al., 1993). It has been assumed that about 50 000 synchronously active cells are needed to generate such magnetic fields (Lopes da Silva, 2010). During a typical evoked response, about a million synapses must be active simultaneously (Hämäläinen et al., 1993).

The equivalent current dipole (ECD) is used to refer to the brain area that contributes most to the measured magnetic field (see 2.2.3). Cortical ECD does not exclude deep triggers, such as those related to thalamic inputs, for the activation of the source area. Measured magnetic field patterns may appear dipolar but this does not indicate that the source is a current dipole. (Hari, 1991)

2.2.2 Instrumentation

As magnetic fields of the brain are very small, they require sensitive instruments for their detection. This sensitivity is obtained by superconductivity, which is at present achieved by bathing the sensors in liquid Helium (the boiling point of Helium is 4.2 K = -269 °C). The superconducting flux transformers detect the magnetic signal and conduct it to the superconducting quantum interference devices (SQUIDs). The SQUIDs in turn convert the magnetic flux into electric voltage. A special container for the liquid helium, known as a Dewar is required to maintain the temperature difference between the head and the sensors.

Most MEG devices use gradiometers to diminish ambient noise. These gradiometers detect the local gradients of the magnetic fields generated by the brain but suppress more evenly distributed artifact fields that originate in the environment. An axial gradiometer consists of a pickup coil and a compensation coil above it (further away from the brain signal). The coils are similar in size but are wound in the opposite directions. This makes the gradiometer less sensitive to background noise as the homogenous fields are effectively cancelled out. The signal that arises near the pickup coil will cause a greater change of the field in the pickup

coil than in the more remote compensation coil (Hämäläinen et al., 1993). The two coils of a planar gradiometer are placed in the same plane. An axial gradiometer obtains the maximum signal on both sides of a current source. A planar gradiometer detects the largest signal over the source (Hari, 1991). The magnetometer is a simple loop that picks up strongest signals when positioned some centimeters away from the source. The magnetometer has a sensitivity pattern that is similar to that of an axial gradiometer (Hari et al., 2010). Nowadays, the sensor arrays cover the whole scalp and the activity of the whole hemispheral cortex can be recorded simultaneously. The Elekta Vectorview™ MEG device used in these studies has 102 triple sensor elements, which include two orthogonal planar gradiometers and one magnetometer. (Figure 3)

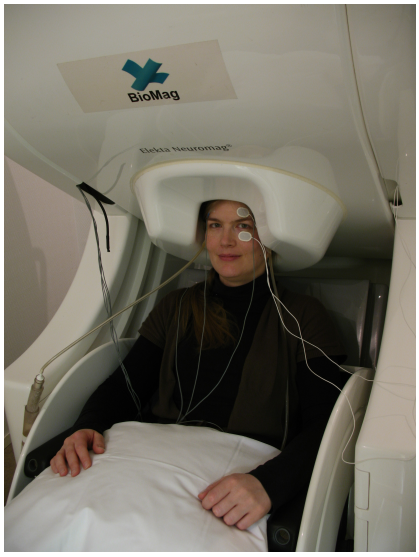

Figure 3. A subject seated under the MEG device in the BioMag Laboratory Helsinki University Hospital.

The recorded signals from the brain are much weaker than the ambient magnetic field alterations. Moving elevators and vehicles, televisions, microwave transmitters, power-lines etc. produce significant ambient magnetic noise. Therefore the MEG devices are usually housed in a magnetically shielded room. The shielding decreases the disruptive signals from outside the room. All possible artifact-producing objects,

moving magnetic materials such as watches, phones, metal components and entities like zips and jewellery must be left outside the shielded room. Even the heart generates a magnetic field, which is two to three times greater in magnitude outside the chest than the brain's magnetic field outside the head (Hämäläinen et al., 1993).

2.2.3 MEG signal modelling

The calculations that are used to model sources of the MEG signal are based on Maxwell's equations, which determine the resulting magnetic field when the electric source current and surrounding conductivity distributions are known. Analyzing measured magnetic fields to resolve the electric source that generates them is called an inverse problem. Theoretically there are an infinite number of sources that could give rise to the measured magnetic field outside the scalp as the solution of inverse problem. The number of possible solutions can be limited to meaningful sources with proper prior knowledge of the source structure. (Hämäläinen et al., 1993) Forward modelling from the calculated source and comparison of the results with the measured magnetic fields is important to evaluate the validity of the results.

The external magnetic flux that is produced by the net intracellular postsynaptic current is directed according to the right-hand rule. Only currents with components that are tangential to the surface of a spherically symmetric conductor generate a magnetic field that can be detected outside the conductor. The corollary of this is that in brain measurements the activity is detected mostly from the fissures of the cortex. Luckily, the primary sensory areas of the brain are to a large extent situated within the fissures (Hämäläinen et al., 1993; Hari and Forss, 1999).

A simple model that is often applied to MEG interpretation is a tangential current dipole within a sphere. The sphere model produces a good enough match to reality in the parietal and occipital areas of the brain, but it does not illustrate the inferior surfaces of temporal and frontal lobes with sufficient accuracy. Realistically shaped head models are needed for brain localities that do not fulfill the presumption of sphericality. (Hämäläinen et al., 1993)

The current dipole that best fits the measured fields is the equivalent current dipole (ECD). It is sought with a least-squares fit to the data. The least-square approach seeks the parameter values that minimize the difference between the observations and the predictions from the corresponding model (Baillet, 2010). Multidipole models can be used to represent complex sources as they can show time-varying source strengths in several locations (Hari, 1991; Hari et al., 2010). The goodness-of-fit (g) value reveals how much of the measured data are explained by the model.

The minimum current estimate (MCE) is a distributed current estimate with the constraint of a minimum norm. The MCE algorithm is based on the l^1-norm, which favours source estimates more focal than the l^2-norm. The l^2-norm is used in minimum norm estimate (MNE). The frequency domain minimum current estimate (MCEfd) enables localization of multiple oscillating sources in a specified frequency band. The signal is first transformed to the frequency domain by dividing it into sections using a sliding window with 50% overlap and using the discrete Fourier transform. The real and imaginary parts of the Fourier transformed signal are used as inputs into the MCE algorithm, which gives current distributions for real and imaginary current sources. The total current estimate is obtained by summing the real and imaginary parts. Then the total current estimates for all the sections are averaged over time, giving a measure of the absolute current density for a given frequency. The MCE results can be spatially normalized to a standard brain, which enables the averaging over many subjects. (Jensen and Vanni, 2002)

In beamforming methods, the brain volume is scanned by sequentially applying spatial filters. A spatial filter sensitizes its output to match the signal from a given brain area (Hari et al., 2010). It separates signals with similar frequency content but different spatial locations. There should not be highly correlated activations in the data analyzed by beamforming method as they are explained by a single source (Baillet, 2010).

The tSSS method (Taulu and Simola, 2006) has been used in the studies described in this thesis for suppressing the huge magnetic artifacts produced by DBS. tSSS is effective in suppressing disturbances from distant and near-by sources. First the measured signal is divided into two spatially separate parts by the signal subspace separation (SSS): one subspace depicts signals from the inside of the sensor array and another one signals that arise outside the helmet (Taulu and Kajola, 2005).

Thereafter, the temporally correlated components within these two subspaces are recognized by principal component analysis and are subsequently removed from the MEG data. The presumption is that the real brain signals are so weak that they do not extend into the outer signal source space. Moreover, the artifacts that arise near the sensor array can be suppressed as they extend into both signal source spaces.

2.2.3.1 Evoked fields

The reactivity of brain activity to stimuli can be studied, inter alia, by using MEG measurements. The MEG response to one stimulus is normally difficult to separate from the background noise. Therefore averaging, time-locked to the stimuli, is needed. Averaging improves the signal-to-noise ratio and as a result the response induced by the stimuli emerges. Often at least 40 – 100 averages are needed to achieve robust evoked fields with an adequate signal-to-noise ratio (Mäkelä, 2014).

The evoked fields elicited by auditory, somatosensory or visual stimuli are used to study the activity of the sensory cortices. For cognitive studies, event-related fields averaged for randomly occurring stimuli, which deviate from the standard stimulus sequence (oddball stimuli), can be measured (Mäkelä, 2014).

The response to sensory stimuli consists of several deflections. The earliest deflections may be separated from each other by only a few milliseconds. These deflections can sometimes be related to separate thalamocortical inputs to different cytoarchitectonic subareas or intracortical transmission (Hari et al., 2010).

2.2.3.1.1 Auditory evoked responses

Auditory evoked fields (AEFs) are elicited by any abrupt sound or alteration in an ongoing auditory stimulus. The most prominent deflection is the N100m response, which peaks about 100 ms after the sound onset or change and has source orientation generating a vertex negative (N) deflection in EEG measurements (Hämäläinen et al., 1993). The response is probably generated in the primary auditory cortex in Heschl's gyrus and posterior to in the supratemporal plane (Hari et al., 2010). The exact

source location depends e.g. on the tone frequency; auditory cortex is thought to be organized tonotopically (Hämäläinen et al., 1993). The AEFs are detected in both hemispheres after stimulus delivery to one ear. The response is stronger and peaks earlier in the hemisphere contralateral than ipsilateral to the stimulated ear. The source of N100m is located about 1.5 cm more posteriorly in the left than right hemisphere (Elberling et al., 1982). Stimulus characteristics modulate the AEFs. The amplitude of N100m increases when the duration of the sound increases from 5 to 20 ms or when the interstimulus interval (ISI) is prolonged up to 8 – 10 s. The N100m amplitude increases and latency decreases by increasing the stimulus intensity up to 90 dB above the hearing level (Mäkelä and Hari, 1990).

The AEFs have been studied in PD patients to investigate the preattentive auditory processing. A significantly prolonged interhemispheric latency difference of P50m and N100m AEFs was observed when the sound was delivered to the left ear (Pekkonen et al., 1998).

The effects of DBS on auditory event-related potentials have been measured by EEG. An auditory oddball paradigm revealed an increase in the N100 latency between on and off DBS states. No significant change was detected in the latency of the P300 response (Naskar et al., 2010). Evidence of involvement of the STN in early-stage auditory processing has been reported in PD patients. Evoked potentials elicited by phonological stimuli were detected from the LFPs recorded in the STN. The effect of levodopa on the subcortical auditory processing was limited (De Letter et al., 2014).

2.2.3.1.2 Somatosensory evoked responses

Human cortical somatosensory organization and processing can be studied by recording somatosensory evoked potentials (SEPs) and magnetic fields (somatosensory evoked fields, SEFs). The SEFs can be elicited by tactile stimulation or by electric pulses to the peripheral nerves. Electric stimuli are widely used as they elicit strong cortical responses although they are not a natural way of activating the sensory cortex (Forss et al., 1994b).

Responses of healthy subjects to median nerve electrical stimuli are well known. The first response, N20m, is elicited about 20 ms after the stimulus in the contralateral primary somatosensory cortex (SI) in Brodmann's areas 3b and 1. The next deflection, P35m, has approximately the same location but an opposite polarity (Forss et al., 1994a). At about 90 milliseconds the secondary somatosensory cortices (SII) are activated in both hemispheres. In general, contralateral SII responses were stronger in amplitude and shorter in latency than the ipsilateral responses. Another activation in the posterior parietal cortex close to the head midline occurs at 70 – 115 ms in most subjects (Forss et al., 1994a). Stimuli delivered at long and random ISIs generate stronger responses. Attention to the stimuli (counting them) increases the response amplitudes (Mauguière et al., 1997).

EEG studies of somatosensory evoked potentials in PD patients are not congruent. Some studies have shown an amplitude decrease in the frontal N30 component (Rossini et al., 1989) but other studies did not confirm this finding (Garcia et al., 1995; Drory et al., 1998). No SEF abnormalities were observed in PD patients with unilateral symptoms (Mäkelä et al., 1993).

Bilateral DBS of both GPi and STN increases the frontal N30 response amplitude but does not modify parietal N20 or P25 deflections; the effect resembles that induced by apomorphine (Pierantozzi et al., 1999). A transient obliteration of post-rolandic SEPs was observed some days after DBS implantation in two patients when the stimulator was not yet on. The amplitude of pre-rolandic deflections was preserved or slightly increased after the commencement of continuous DBS (Insola et al., 1999). Recordings of DBS effects on SEPs were taken after discontinuing DBS in both studies.

2.2.3.2 Spontaneous brain oscillations

Brain electrical activity is characterized by rhythmic oscillations, with frequencies that range from infraslow (below 0.1 Hz) frequencies up to 600 Hz oscillations (Mäkelä, 2014). The most studied brain rhythms include occipital alpha and rolandic mu rhythms. Sources of temporal 10-Hz oscillatory activity (“tau rhythm”) are located near the sources of auditory evoked responses (Hari et al., 1997). These rhythms can be

modified separately by voluntary actions such as closing the eyes, or making hand movements.

2.2.3.2.1 Occipital alpha rhythm

The peak frequency of the occipital alpha rhythm is around 10 Hz. Its sources, detected by MEG, cluster around the parieto-occipital sulcus and around the calcarine sulci. The occipital alpha rhythm is suppressed by opening the eyes. Dampening of the occipital alpha rhythm also occurs after visual stimulus and even after mental imagery of an image. (Hari et al., 1997)

2.2.3.2.2 Mu rhythm

The rolandic mu rhythm consists of frequencies at about 10 and 20 Hz; the combination of these frequencies creates the typical 'comb-like' shape of these oscillations. The mu rhythm is dampened by movement, by preparing to initiate a movement or by imagining a movement. Tactile stimuli suppress the mu rhythm (Salmelin and Hari, 1994). Practically all healthy subjects display MEG oscillatory activity at these frequencies, at least after executing a movement (Hari et al., 1997).

The rebound after movement-induced suppression is faster and stronger for the 20 Hz component (Hari et al., 1997). The sources of the 20-Hz signals tend to cluster anterior to the sources of the 10 Hz signals. The 20-Hz oscillations are presumed to be generated in the sensorimotor cortices whereas the 10-Hz rhythm may be predominantly generated in the somatosensory region (Salmelin and Hari, 1994).

2.2.3.3 Coherence

Coherence is a measurement of the linear dependence of two signals and describes the relationship between two time series. It is defined as the magnitude of the squared cross spectrum of the two signals normalized by the power spectra of both time series at a given frequency bin. The coherence values vary between 0 and 1, and reflect the consistency of the phase difference between the two time series; 0 indicates no resemblance

between the two time series, whereas 1 indicates a perfect linear association. The classical coherence measures have some limitations. For example, data must be stationary. Coherence between two signals can also result from a common input from a third signal. Coherence is also sensitive to both the amplitude and phase dynamics. (Gross et al., 2010)

2.2.3.3.1 CMC

The first observations that muscle discharge is likely to be rhythmic was made 200 years ago by William Wollaston. Later, in the beginning of 20th century, Hans Piper described a modulation of motor unit discharge at around 40 Hz. The first evidence supporting a central origin for this motor unit synchronization was presented in the early 1990s. (Grosse et al., 2002)

CMC is thought to indicate the co-ordination between cortex and muscle during static motor activity. The CMC activity is estimated between simultaneously recorded MEG / EEG and by electromyography (EMG) signals. There is a consistent phase lag between the motor cortex (M1) and EMG signals (M1 activity preceding EMG) and it is therefore thought that the motor cortex drives the spinal motoneuron pool (Gross et al., 2000). The cortical rhythm probably tunes the activity of a population of motor units (MUs) instead of driving individual MUs (Hari and Salenius, 1999). Recently, sensory feedback from the periphery has also been suggested to contribute to CMC (Witham et al., 2011). The beta frequency band (13 – 35 Hz) of the brain signals is most often coherent with EMG during the maintained motor task. Signals in the alpha (around 10 Hz) or gamma (40 – 50 Hz) frequency bands display coherence only occasionally (Conway et al., 1995). The CMC in the gamma band is more obvious during strong muscular contractions (Brown et al., 1998). The CMC sources for hand and foot muscle activation display a crude somatotopic organization in the contralateral motor cortex. Nevertheless, there is no difference in the sites of maximum coherence between the various upper limb muscles (Hari and Salenius, 1999).

The level of coherence during a precision grip task is influenced by the task features (Kilner et al., 2000). Precise motor performance may (Kristeva et al., 2007) or may not (Johnson et al., 2011) correlate with high CMC values. Divided attention during muscle activation decreases

CMC amplitude (Kristeva-Feige et al., 2002; Johnson et al., 2011). The intra-session reproducibility of CMC strength and peak frequency has reported to be good (Pohja et al., 2005).

The 40-Hz Piper rhythm, detected during strong wrist extension was replaced in PD patients by pulsatile muscle activity of about 10 Hz during an off medication period. Subsequent dopaminergic medication restored the piper rhythm, indicating the importance of the proper functioning of pallidal projections to the motor cortex for normal muscle discharges. (Brown, 1997.)

The CMC in the 15 – 30 Hz band during isometric contraction was found to be weaker in PD patients withdrawn from levodopa treatment compared with healthy controls. Levodopa treatment was also reported to increase the CMC in PD patients (Salenius et al., 2002). However, CMCs of the de-novo PD patients or early-stage PD patients had similar CMCs compared with healthy controls (Pollok et al., 2012). The CMC amplitude between sensorimotor MEG signals and the muscle of the tremorous hand in the range of 10 –30 Hz increased during STN-DBS in three PD patients. This increase correlated with decrease of UPDRS tremor points (Park et al., 2009). A study on eight PD patients found that the average EEG-EMG CMC in the 15 – 20 Hz range was slightly increased eight days after DBS implantation when DBS was switched on (Weiss et al., 2012).

Parkinsonian resting tremor also creates CMC at the tremor frequency and at its harmonics (Volkmann et al., 1996; Timmermann et al., 2003). MEG recordings and data analysis with dynamic imaging of coherent sources (DICS) suggest a network comprising primary sensorimotor cortex, premotor cortex, cerebellum and thalamus that are activated during the resting tremor (Schnitzler et al., 2006). The oscillatory network observed in healthy subjects with mimicked resting tremor is to a large extent similar to that observed in PD patients during tremor (Pollok et al., 2004). In an MEG study of one patient, DBS suppressed resting and postural tremor and CMC at 4 -Hz tremor frequency and at 8 Hz (Connolly et al., 2012).

2.2.3.3.2 CKC

Corticokinematic coherence can be estimated between simultaneously recorded MEG and accelerometer signals from a moving body part. The CKC is found at the movement frequency and its first harmonic (Bourguignon et al., 2011; Piitulainen et al., 2013a, 2013b), and sources of CKC are localized in the sensorimotor cortex contralateral to the moving body part (Bourguignon et al., 2011). A comparison of active and passive finger movements suggested that the CKC that arises during repetitive finger movements is driven mainly by proprioceptive afferent input to the primary sensorimotor cortex (Piitulainen et al., 2013b).

3. AIMS OF THE STUDY

The aim of this study was to explore the effects of DBS on the brain electrical activity in advanced PD patients with the ultimate aim of gaining a better understanding of its therapeutic mechanisms. The patient data made evident the need to understand better the physiological mechanisms of CMC. Study IV in healthy volunteers describes the first step in this endeavour. The specific goals were:

1. Confirm that the MEG data obtained from DBS treated patients is amenable to analyses after artifact rejection by tSSS. Previously well known SEFs and AEFs were analyzed to see if DBS artifacts can be removed efficiently and if the remaining signals contain physiologically valid data (Study I).

2. Study the effects of DBS on spontaneous brain rhythms in PD patients (Study II).

3. Investigate the effect of DBS on CMC in PD patients (Study III).

4. Compare CMC and CKC during static muscle contraction in healthy volunteers to gain a better understanding of the physiology of CMC (Study IV).

4. MATERIALS AND METHODS

4.1 Patients and Subjects

A total of 24 advanced PD patients who were treated with STN-DBS (Kinetra or Activa PC Neurostimulators, Medtronic Inc, Minneapolis, MN, USA) were recorded by MEG in studies I – III.

The patients were recruited from the Department of Neurology in Helsinki University Hospital. The mean age of the patients was 59 years (± 10 years). The patients had had their diagnosis about 13 years (± 5 years) before DBS implantation. Their mean UPDRS motor III scores during the MEG recordings were 22.7 (± 11.5) when DBS was on and 36.7 (± 17) when DBS was off ($p < 0.001$). The mean levodopa equivalent daily dose (LEDD) was 1020 mg (± 495 mg) (Table 1). The following formula was used to calculate the LEDD: 100 mg levodopa = 130 mg controlled-release levodopa = 70 mg levodopa + COMT inhibitor = 1 mg pramipexole = 5 mg ropinirole (Mamikonyan et al., 2008) = 4 mg rotigotine (Poewe et al., 2007).

Study I reports data from 12 patients. The same patients participated in Study II; one of them was excluded because of missing UPDRS scores when the DBS was off. Study III reports data from 19 patients, 7 of whom had also been included in Study I. The other 12 patients had not participated in any previous study. Four patients of Study I were excluded because their MEG measurements were taken less than two months after the DBS implantation.

All patients used their regular antiparkinsonian medication during the MEG recordings. The UPDRS III motor scores in studies I– III were determined before the patient entered the shielded room with DBS on and when the patient exited the shielded room after the measurement when the DBS had been turned off.

Data of some patients measured with MEG were excluded from the reports. In one patient, strong artifacts saturated the MEG amplifiers completely and no brain signals were recorded. In another patient, localization of the head position failed. A few patients did not tolerate the measurements during the DBS off phase. Another subgroup of patients

was excluded due to missing UPDRS scores or small, ineffective DBS voltages.

Table 1. Patient characteristics.

Patient	Sex	Age	Disease duration before operation (years)	Time since stimulator implanted (months)	UPDRS		LEDD (mg)	Participated in Study
					DBS on	DBS off		
1	M	59	14	25	23	31	2160	I – III
2	M	59	11	24	17	20	1290	I – III
3	F	60	7	25	39	49	620	I – III
4	M	68	10	7	27	37	490	III
5	M	36	8	4.5	26	71	210	III
6	M	43	10	6	21	60	570	III
7	M	63	18	5	20	21	1550	III
8	M	57	16	6		19	1260	III
9	F	68	14	5	44	69	530	I – III
10	M	49	9	25	16	25	1600	I – III
11	M	42	6	6	6	17	1660	III
12	F	64	25	7.5	18	40	650	III
13	M	68	21	17	30		1650	I, III
14	M	58	12	24	33	38	1200	I – III
15	M	64	9	6.5	22	38	560	III
16	F	66	18	6	10	20	850	III
17	M	47	8	6	6	45	460	III
18	M	50	14	12	18	24	1080	III
19	M	71	8	6	12	27	820	III
20	F	67	11	2	12	14	1120	I – II
21	F	55	19	1.5	22	60	1170	I – II
22	F	65	10	1	16	23	1060	I – II
23	M	60	16	0.5	34	46	1500	I – II
24	F	75	13	1.6	50	50	510	I – II

In Study III, subgroup analyses were done for 10 patients with more than 30% decrease in UPDRS III motor scores when DBS on to study the robust effect of DBS on motor symptoms.

Ten healthy subjects (4 female, mean age 30 years, range 22 – 58 years) participated in Study IV.

The research protocols for all four studies were accepted by the Ethics Committee of the Department of Neurology, Helsinki University Hospital. All patients and subjects gave their informed written consent.

4.2 MEG measurements

The MEG was recorded in the BioMag Laboratory of Medical Imaging Center, Helsinki University Hospital by a 306-sensor Vectorview™ neuromagnetometer (Elekta Neuromag®, Elekta Oy, Helsinki, Finland) with 204 planar gradiometers and 102 magnetometers. The MEG device was situated inside a magnetically shielded room (Euroshield Ltd., Eura, Finland).

The alignment of the MEG and magnetic resonance imaging (MRI) co-ordinate systems was done by placing the head position indicator coils with respect to head landmarks using a 3-D digitizer (Fastrak®, Polhemus, Colchester, VT) and activating the coils before each measurement. Each patient's head position with respect to the MEG helmet was determined at the commencement of recording in studies I–III. The head position of healthy subjects was recorded continuously in Study IV.

The patients were recorded first with DBS on and then with DBS off. This sequence was reversed for one patient. An experienced nurse was in the shielded room with the patient to monitor their welfare and performance and control alertness.

The auditory stimuli were delivered by Presentation software and directed through plastic tubes to the patient. The delay caused by the tubes was taken into account in the analyses. AEFs were elicited by sinusoidal 1-kHz 50-ms tone pips. Stimulus intensity was about 60 dB above the ambient noise. The sounds were delivered to each ear separately. We confirmed that the patients heard the tone pips clearly.

Electrical stimulators (Digitimer Ltd, model DS7A, Welwyn Garden City, England) were used to produce electrical 200-μs square-wave pulses for

median nerve stimulation. They were delivered alternately to both median nerves with intensities sufficient to elicit a clear but non-painful thumb twitch.

Visual checkerboard stimuli were also presented to the patients but the results were not analyzed further. Auditory, somatosensory and visual stimuli were displayed in random order in one stimulus sequence. The time between subsequent stimuli was 600 ms. The minimum ISI was 0.6 s and the mean ISI 5.5 s for each stimulus type.

Spontaneous MEG was recorded first with the eyes closed for three minutes and then with the eyes open for five minutes both when DBS was on and off.

Bipolar EMG recording were taken by attaching surface electrodes over the extensor carpi radialis muscle. The EMGs of patients were recorded from the more affected upper limb. The EMGs were recorded from both forearms of healthy volunteers. Horizontal and vertical electrooculography (EOG) was recorded to enable exclusion of eye movement and blink artifacts. The recording passband was 0.03 – 330 Hz and the sampling rate 1012 Hz for MEG, EMG and accelerometer signals.

The patients (Study III) and subjects (Study IV) were requested to extend their wrist (dorsiflexion) five times for one minute. Each dorsiflexion was separated by a 20-s rest period. The patients in Study III extended the more affected hand. Volunteers in Study IV extended first the right hand and then the left hand.

Postural tremor in Study IV was recorded using an accelerometer (ADXL335 iMEMS Accelerometer, Analog Devices Inc., Norwood, MA, USA). The movement sensor was fixed onto the fingernail of the index finger of both hands. The accelerometer measures finger acceleration in three orthogonal directions.

4.3 Data analyses

DBS produced strong magnetic artifacts which were suppressed by the tSSS method (Taulu and Simola, 2006) (Figure 4). An 8-second time

window and a subspace correlation limit of 0.9 (Studies I, III and IV) or 0.8 (Study II) were applied.

The EMG in Study III was rectified before subsequent analyses. The EMG in Study IV was not rectified.

The sensor positions were equalized by applying the multipole-based method (Taulu et al., 2005) implemented in Elekta MaxFilter™ software to enable the comparison between DBS on and off conditions in Study III.

4.3.1 Dipole modelling

Source analyses in Study I were done with an ECD model. The applied spherical head model was fitted into the individual brain MRIs. Two patients did not have a brain MRI. For them, the x-, y-, and z-co-ordinates of 0, 0, 40 mm were used as sphere origin. The responses were averaged from tSSS-processed raw data. AEFs were filtered with a 1 – 40 Hz passband. For SEFs, the passband was 0.5 – 100 Hz.

The sources of the AEF N100m were sought from hemispheres contralateral and ipsilateral to the stimulated ear. A subset of 11 – 15 gradiometer pairs around the maximum response was used in the source localization. ECDs were fitted with a 1-ms interval sequentially 80 – 130 ms after the stimulus onset. Co-ordinates of the best dipoles (in terms of source strength and goodness-of-fit) for auditory cortex source for each patient were selected and used to calculate time-varying N100m source strengths with DBS on and then off.

The sources of SEFs were estimated by sequential ECD fitting with 1-ms intervals 15 – 80 ms after the stimulus. Twelve to fourteen gradiometer pairs around the maximum response were used to calculate the SEF sources in the primary somatosensory cortex (SI) contralateral to the stimulus. The ECDs were determined when DBS was on and then off. Co-ordinates of the best dipoles were selected for each patient with the same criteria as in AEFs. The source strengths and latencies of N20m and P60m were determined from dipole strength versus time curves for both the DBS on and off conditions.

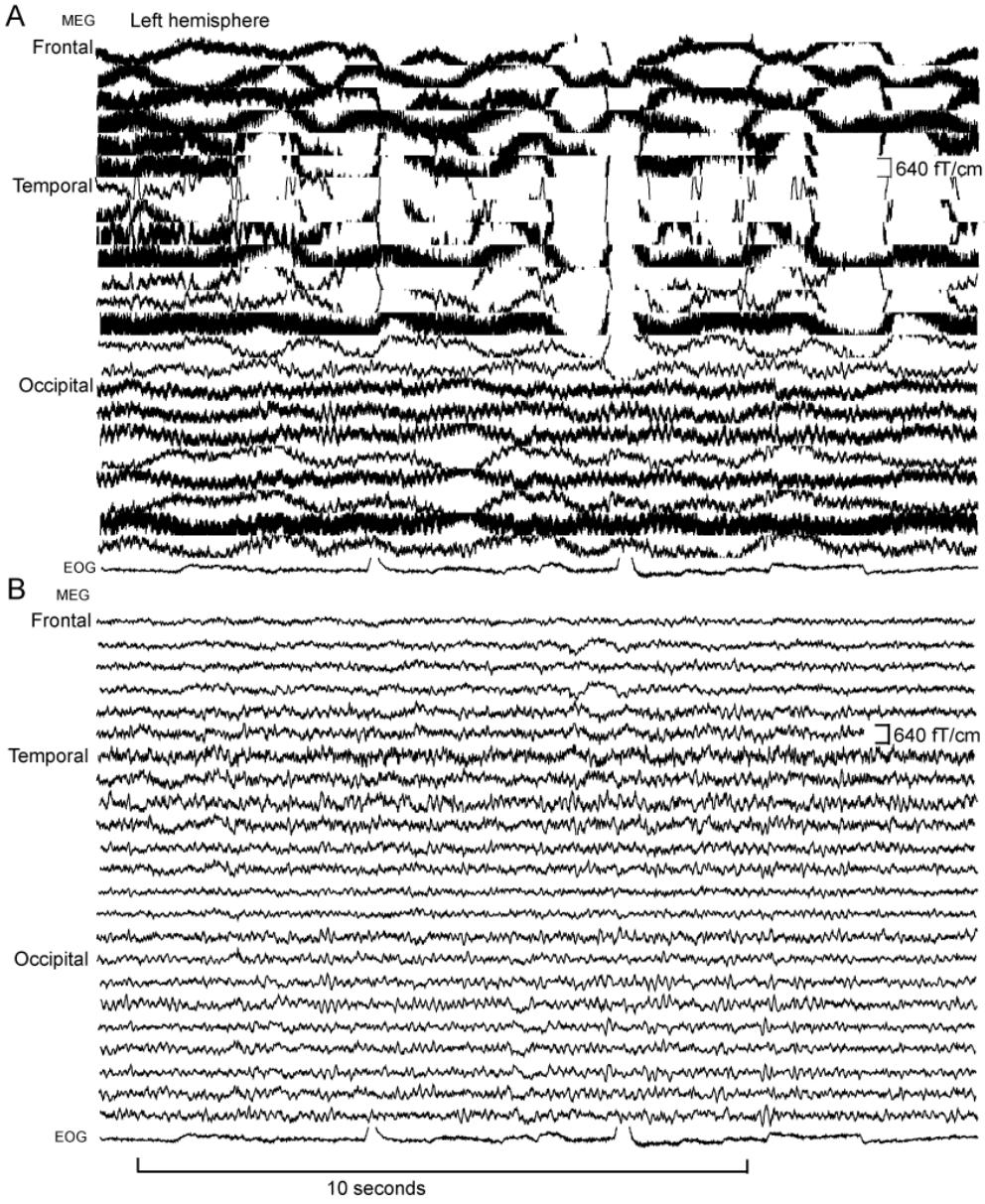

Figure 4. Spontaneous recordings of MEG from the left hemisphere and EOG recording when DBS on. A before tSSS; B after tSSS. Data from Study I.

4.3.2 Analysis of spontaneous brain activity

The sources of oscillatory activity in Study II were localized by the frequency domain minimum current estimate (MCEfd) (Jensen and Vanni, 2002). The fast Fourier transform (FFT) spectra were calculated from the signals to detect any interesting spectral ranges. The FFT length was 512 samples corresponding to a frequency resolution of about 2 Hz. The spectral peaks were carefully inspected. Although the tSSS suppressed most DBS artifacts, some narrow interference peaks remained in the spectra. The lowest detected artificial peak was at 20.7 Hz. Signals at spectral ranges of 2 – 6 Hz, 6 –10 Hz, 12 – 20 Hz and 21 – 30 Hz in the sensorimotor region were selected for the study. The 20 – 21 Hz band was omitted from further analyses because of the spurious artifact peak at 20.7 Hz. The individual mu rhythm frequency band around 10 Hz (peak ± 2 Hz) was examined as well. The source amplitudes in the occipital region were studied from a frequency band around the individual peak alpha frequency ± 2 Hz.

In MCEfd, the data are transformed to a frequency domain using the discrete Fourier transform (DFT). A DFT segment size of 4096 samples was used to obtain 0.25 Hz frequency resolution. The minimum current estimate (MCE) was made for the transformed data (Uutela et al., 1999).

A region of interest (ROI) was outlined over the active source areas. The ROI was fitted automatically for each subject. The total source amplitude was computed from a weighted sum of all active voxels of the ROI. The weighting function was a three-dimensional Gaussian, with a magnitude of 1 at the center of the region and 0.6 at the edge (Jensen and Vanni, 2002). The same ROIs were used for data recorded with DBS in the on and off conditions.

4.3.3 Power spectral density

Power spectral densities (PSD) of MEG, EMG and accelerometer signals were estimated for each subject using Welch's method with 50% overlapping 1024-point Hanning windows, which resulted in a frequency resolution of approximately 1 Hz. The PSD in Study III was normalized by dividing it with the average PSD between 3 and 48 Hz. The grand averages were calculated by averaging these normalized PSDs over the

patients. The average spectra for DBS on and off conditions were compared for 6 – 13 Hz and 13 – 25 Hz bands.

The EMG signal was high-pass filtered above 0.5 Hz, rectified, and then averaged with a 51-point moving average filter to analyze the stability of EMG in Study III. The following equation was used (Lim et al., 2011):

$$\text{Stability of EMG} = 1-(SD(EMG_{\text{rectified and averaged}}) / \text{Mean}(EMG_{\text{rectified and averaged}}))$$

The stability was averaged across all epochs of EMG to obtain individual EMG stability values. This was done separately for DBS on and off conditions.

4.3.4 Coherence analysis

Sensor level CMC was estimated between the EMG and MEG signals in Study III. The coherences in Study IV were estimated between three different signal types: MEG, EMG and accelerometer signals. For three orthogonal accelerometer channels, we used a signal corresponding to the greatest singular value based on the singular value decomposition

4.3.4.1 Sensor-level coherence

The sensor-level coherence was estimated between the EMG or accelerometer signal and signals from each MEG gradiometer pair in turn. Welch's method with 50% overlapping 1024-point Hanning windows (frequency resolution about 1 Hz) was applied. The number of averaged segments used for coherence calculations varied (range 106 – 618; mean in Study III 451 ± 118 and in Study IV 556 ± 54). The time segments in Study IV were same for EMG and accelerometer data.

The location of the CMC / CKC maximum peak was established by visual inspection from 15 selected gradiometer pairs for the sensorimotor cortex contralateral to the activated hand. Peak strengths and frequencies were determined from this maximum peak.

The coherence spectra in Study III were divided into 4 – 6 Hz, 6 –13 Hz and 13 – 25 Hz frequency bands. A more detailed examination of the

patients with CMC in the 13 – 25 Hz band was carried out by dividing the patients into three groups. One group had significant CMC both in DBS on and off conditions; one group did not have any CMC in either condition, and one group had significant CMC when the DBS was either on or off.

4.3.4.2 Source-space coherence

The MRILab software (Elekta Oy) was used to co-register MEG with an anatomical MR image, aligning co-ordinates of the head and the MRI. The FreeSurfer software (MGH, Boston, MA) or Seglab software (Elekta Oy) was used for MR image segmentation. The segmentation separates the brain from the surrounding tissue, thus providing a volume for possible sources.

The Dynamic Imaging of Coherence Sources (DICS) method in Beamformer software (Elekta Oy) was used for source-space coherence estimation in Study IV. The sensor-level CMC and CKC peaks were used as the basis for selecting 6-Hz frequency bands for coherence estimation, and all further analyses were restricted to this band. An evenly distributed grid of locations that covered the brain volume with a resolution of 3 mm was used. Only the direction that had maximum power was used for each location. A virtual electrode signal (estimate of source activity in the time domain) was estimated from the location of maximum coherence after the beamformer coherence scanning. The final CMC and CKC results were computed using these virtual electrode signals.

4.3.5 Statistical analyses

SPSS (SPSS for Windows version 13.0 or 17.0, SPSS, Chicago, IL) was used for statistical analyses. The results are reported as means ± standard deviations when appropriate. The level of statistical significance was set for p-value below 0.05.

Time-shifted coherence (coherence calculated by shifting EMG data 3 seconds in relation to the MEG data) was used for testing the statistical significance of the sensor-level coherence. Any true coherence in these

data was presumably destroyed by the shift. The significance level was set at 99% of the time-shifted coherence (Salenius et al., 2002).

Comparisons of the DBS on and off states data within individuals in Study I were made using the paired t test. The statistical comparisons in Studies II, III and IV between two dependent groups were analyzed by Wilcoxon Signed Ranks Test. The comparisons between three different groups in Study III were analyzed by the Kruskal-Wallis test and Dunn's multiple comparison tests. The Mann-Whitney test was used for comparison of the distributions of two independent groups (Study III). Spearman correlation was used in Studies II, III and IV to calculate the significance of correlations.

The x-axis co-ordinates in Study IV were transformed to positive values (absolute values of the x-co-ordinates) for statistical calculations and a one-sample t-test was used for the calculations of significance for co-ordinate differences.

5 RESULTS AND DISCUSSION

5.1 Feasibility of MEG in studies of the effects of DBS (Studies I – III)

Carrying out studies of the effects of DBS on brain electrophysiology is challenging. Devices that are used for DBS are magnetic; patients that have DBS battery implants cannot be studied with functional MRI, and transcranial magnetic stimulation (TMS) of these patients can be hazardous. DBS, on the other hand, does not complicate PET or single photon emission computed tomography (SPECT) studies. PET and SPECT, however, produce only indirect measures of neural activity as they explore the changes in blood flow or metabolism. Moreover, their temporal resolution is not good enough to study brain oscillations. Repeated PET or SPECT measurements may also expose the patient to the effects of excessive radiation.

EEG and MEG are non-invasive methods with high temporal resolutions. DBS can cause huge electrical /magnetic artifacts that may mask all measurable brain signals. This confounding property has hindered both the use of EEG and MEG in this field. The tSSS method, fortunately, provides robust artifact suppression for MEG data and we wanted to study its usefulness with DBS studies.

The artifact suppression used In Study I was accurate enough to enable evoked field studies. The patients had the connecting wires and the battery placed on the left side, which resulted in stronger artifacts over the left hemisphere; consequently, signal-to-noise ratio was better in the right than left hemisphere. Adequate contralateral N100m responses were found from 10/12 right and from 8/12 left hemispheres. The P60m SEF responses were detected from 11/12 right and 10/12 left hemispheres. The N20m SEFs were found only in 3/12 of the left and 9/12 of the right hemispheres. Both AEFs and SEFs corresponded in form, timing and location to those reported previously for healthy subjects. The variance of the results may have been increased by any artifacts that remained in the data even after tSSS. Indeed, if the recording amplifiers were saturated by the DBS artifacts during the measurement, no brain data would be captured and artifact suppression methods could not restore those data.

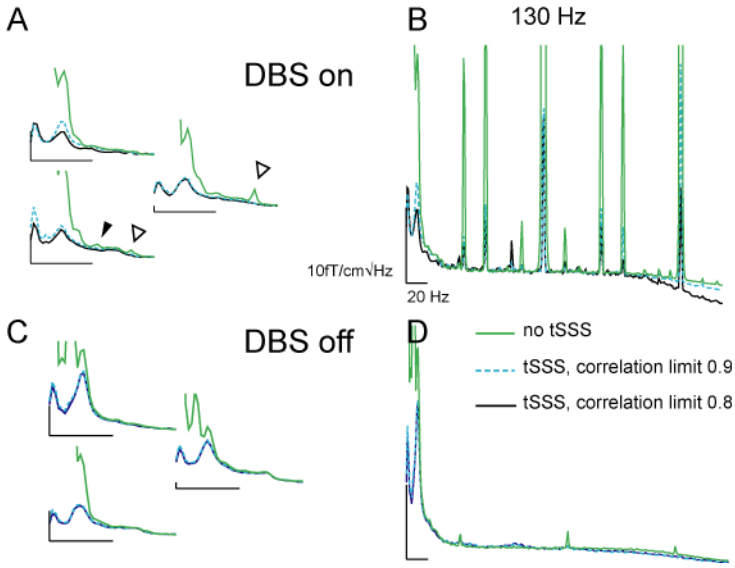

Figure 5. The amplitude spectra of spontaneous brain activity. The band in the right-side (B and D) image shows spectra for the 0 – 300 Hz frequency range, upper figure (A and B) shows DBS on, and lower figure (C and D) shows DBS off. On the left side (A and C) spectra from one sensor triplet in the 0 – 40 Hz band. The green line is the spectrum without tSSS, the dashed blue line shows the spectrum after tSSS with correlation limit of 0.9 and black line after tSSS with correlation limit of 0.8. The artifact peaks produced by the DBS are clear when the DBS was on. The peaks appear symmetrically around the stimulation frequency of 130 Hz. A: tSSS does not totally remove the DBS artifact peaks at 20.7 Hz (black arrowhead) or 32.4 Hz (open arrowhead). D: When DBS is off, the mains 50 Hz artifact and its harmonics can be detected. C: tSSS adequately suppresses the low frequency artifacts that are also present when DBS is off. They arise from the wires and battery when they are moved e.g., by movement of the chest due to respiration. Modified from Study II.

Spontaneous data analysis was fraught with more problems. The tSSS method effectively suppressed most DBS artifacts, but some narrow interference peaks were left in the spectra, particularly when the DBS was on (Figure 5). One of these artificial peaks was found at 130 Hz, at the rate of DBS. Additional artifact peaks spread symmetrically above and below the stimulation frequency. The lowest artifact peaks were found at 20.7 Hz and 32.4 Hz but were not totally erased by tSSS. Artifacts were more robust in the left than right hemisphere, above the wires that connected the DBS battery to the electrodes. Monopolar stimulation produced stronger artifacts than the bipolar stimulation. The DBS probably produces some high-frequency interference that is not sufficiently suppressed by the applied anti-aliasing filters of the used

MEG device. An aliased DBS-interference component, however, did not completely explain the artificial spectral peaks in our phantom experiments (see 6. Additional Material).

5.2 DBS effects of evoked fields (Study I)

The AEF N100m response to right-ear stimulation was significantly enhanced in the right hemisphere (49 ± 17 nAm DBS on, 43 ± 16 nAm DBS off: $p < 0.05$). The contralateral N100m mean source strengths increased non-significantly when DBS was on (left hemisphere: 47 ± 22 nAm DBS on, 44 ± 19 nAm DBS off and right hemisphere: 61 ± 26 nAm DBS on, 58 ± 22 nAm DBS off) (see Figures 6 and 7).

The SEF source strengths were non-significantly increased when DBS was on. The AEF and SEF response latencies were not modified by DBS.

5.2.1 Discussion of Study I

The AEF N100m amplitude at the group level increased significantly in the right hemisphere for ipsilateral stimulation. The worse data quality was found in the left hemisphere. This was probably due to left-sided electrode leads in most patients. Hence DBS artifacts may have masked the effect in the left hemisphere. The ipsilateral auditory pathways from the inner ear to the cortex through the thalamus are thinner than contralateral ones. The ipsilateral auditory pathways are thus possibly more sensitive to DBS effects than the contralateral pathways. We did not find an effect of DBS on latencies of N100m as reported in auditory event-related potentials elicited by an oddball paradigm (Naskar et al., 2010). Naskar and collagues applied auditory stimuli bilaterally; consequently, ipsilateral and contralateral responses were not examined in their study. The alpha-band coherence between STN and superior temporal gyrus (including the auditory cortex) has confirmed a connection between the two areas (Hirschmann et al., 2011; Litvak et al., 2011).

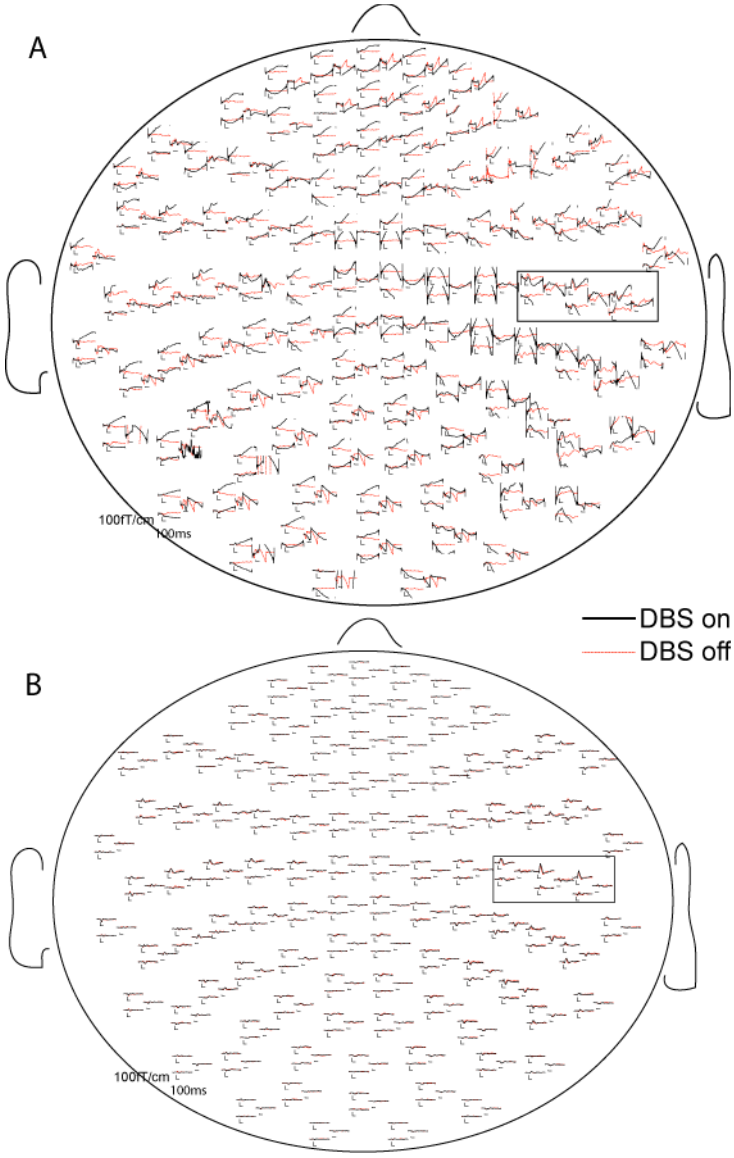

Figure 6. AEFs of one patient before (A) and after (B) tSSS. The responses are shown from above, with the patient's nose pointing upwards. The black line shows DBS on and the red line shows DBS off. The stimulus was delivered to the right ear, inducing the strongest responses in the left hemisphere. AEFs in the squares are shown in Figure 7. Modified from Study I.

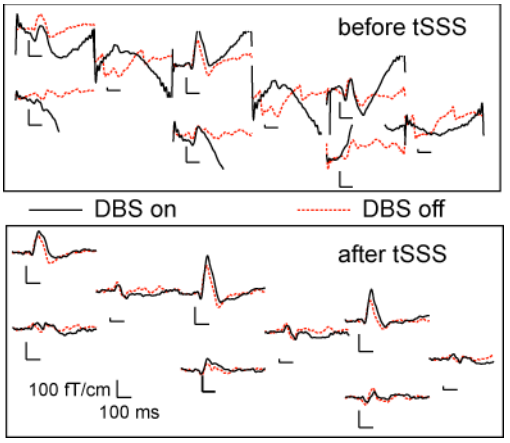

Figure 7. AEFs of one patient selected from the whole-head data in Figure 6 and shown in enlarged form. The upper box depicts data before and the lower box after the tSSS. The black line shows DBS on, red dotted line shows DBS off. The strongest deflection peaks at 100 ms (N100m). Modified from Study I.

No significant differences were found in the SEFs between DBS on and off conditions. The previously reported effects of DBS on somatosensory evoked potentials were not totally uniform (Pierantozzi et al., 1999; Priori et al., 2001). In our study considerable inter- and intraindividual variation of the DBS effects and also the antiparkinsonian medication during the measurements might have influenced the results.

The effects of DBS on SEFs and AEFs were modest but the observed changes suggest that STN-DBS modifies the thalamocortical pathways and / or cortical processing. The effect of DBS on late evoked potentials also supports the notion that a proportion of the DBS effects take place at the cortical level.

5.3 DBS effects on spontaneous brain rhythms (Study II)

The effect of DBS on 10 and 20 Hz spontaneous cortical activity was very variable. Depending on the individual, the signal strength could be stronger or weaker when DBS was on vs. off. When DBS was turned on, group level results of the source strengths of pericentral cortical regions revealed a non-significant decrease in the 6 – 10 Hz band, around the

individual mu rhythm peak in the 5 – 11 Hz range, and in the lower and higher beta ranges (Figure 8).

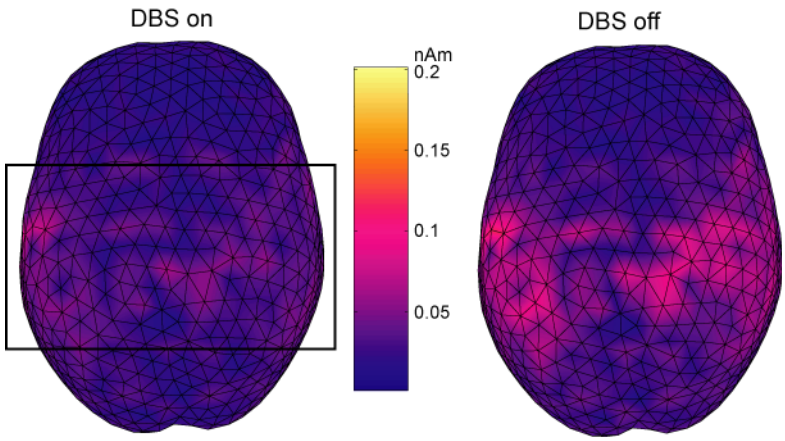

Figure 8. Sources of spontaneous 12 – 20 Hz brain activity with eyes closed for both the DBS on and off conditions. The frequency domain Minimum Current Estimates averaged over four patients with 20-Hz activity increased in the pericentral region when DBS was off. The ROIs were formed individually for each patient using the area that is marked with the rectangle on the left. Modified from Study II.

The peak frequencies of occipital alpha rhythm varied between 5.7 Hz and 10.9 Hz. When eyes were closed and DBS was turned on the source strengths around the individual peaks (± 2 Hz) decreased from 7.6 nAm to 7.1 nAm ($p = 0.05$). When the patients' eyes were open the source strengths decreased from 6.2 to 5.7 ($p = 0.33$).

5.3.1 Correlation of the spontaneous brain rhythms with the motor state

The source strengths of the 6 – 10 Hz and 12 – 20 Hz signals and the source strength of the peak frequency in the 5 – 11 Hz band in the pericentral region correlated with coefficients from a minimum of 0.65 ($p = 0.03$) with UPDRS rigidity subscores when the patients' eyes were open and DBS was on (Table 2, Figure 9).

Correlations between UPDRS action tremor scores and pericentral 6 – 10 Hz and 21 –30 Hz source strengths and the source strength of peak frequency in the 5 – 11 Hz band were seen, when DBS was off (Table 2, Figure 9). These correlations were particularly marked when the eyes were open.

Table 2. Spearman correlations between the pericentral signal source strengths and UPDRS rigidity or action tremor subscores when the patients' eyes were open.

Frequency band	UPDRS rigidity (DBS on)	UPDRS action tremor (DBS off)
	Spearman's rho	
6 – 10 Hz	0.0687 (p = 0.019)	0.645 (p = 0.032)
12 – 20 Hz	0.0668 (p = 0.025)	0.565 (p = 0.070)
21 – 30 Hz	0.510 (p = 0.109)	0.782 (p = 0.004)
5 – 11 Hz peak	0.748 (p = 0.008)	0.673 (p = 0.023)

The individual peak frequency in the 5 – 11 Hz band in the pericentral region correlated negatively with rigidity subscores when eyes were closed and DBS was off (r_s = -0.735, p = 0.01).

Occipital alpha activity source strength correlated significantly with UPDRS action tremor scores when DBS was off particularly when eyes were open (r_s = 0.848, p = 0.001) (Figure 9).

The peak frequency of occipital alpha had negative, significant correlation with UPDRS total motor scores (DBS on: r_s = -0.621, p = 0.041, DBS off: r_s = -0.689, p = 0.019) and rigidity subscores (DBS on: r_s = -0.646, p = 0.032, DBS off: r_s = -0.711, p = 0.014) when the eyes were closed.

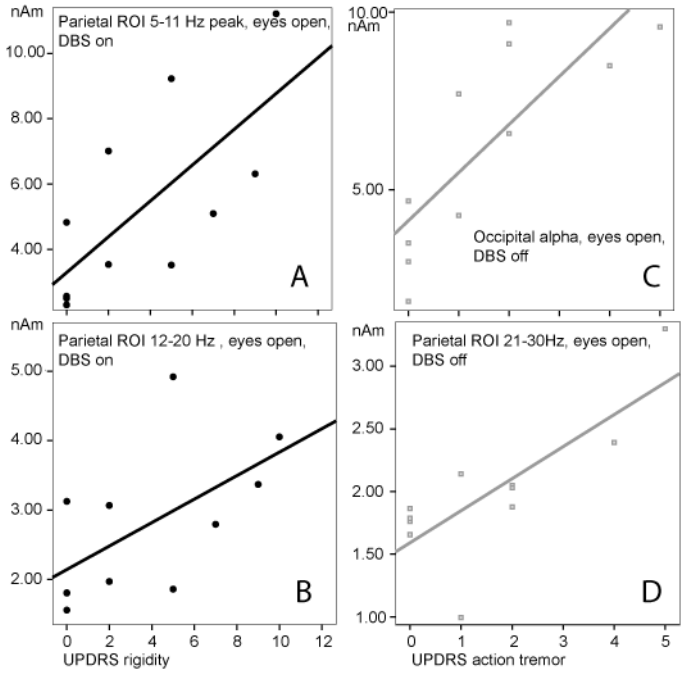

Figure 9. Scatterplots of UPDRS rigidity (A, B) and action tremor (C, D) scores and source strengths of spontaneous brain activity with eyes open from parietal ROI at peak (±2 Hz) frequency in the 5 – 11 Hz range (A), and in the 12 – 20 Hz range (B) and from occipital ROI at alpha (C) and from parietal ROI in the 21 – 30 Hz range (D). A and B: DBS on (black line); C and D: DBS off (grey line). Modified from Study II.

5.3.2 Discussion of Study II

The DBS effect on spontaneous MEG of individual patients varied considerably. DBS decreased the oscillatory beta activity over the sensorimotor cortex on the group level but this effect was non-significant. Increase of beta band activity elicited by DBS over the whole cortex has been reported (Cao, 2015). Several reasons may explain this difference between the two studies. Patients that were studied by Cao were recorded without simultaneous medication and they had already received a longer DBS treatment at the time of the MEG measurements. Moreover, only sensor space data from magnetometers were reported in Cao's study. In both studies some frequencies had to be omitted from the analysis because of artifact peaks.

The DBS effect on cortical beta activity may well be more complex than uniform modulation of its strength. A study of cortical phase-amplitude coupling of electrocorticography (EcoG) recorded from the motor cortex of PD patients going through DBS implantation, before, during and after STN stimulation, found both increases and decreases in cortical beta power due to DBS (de Hemptinne et al., 2015). The authors noted, however, that all patients had a significant decrease of phase-amplitude coupling between cortical beta band and broadband signals during DBS. They also noted a difference between the effect of DBS on beta power in the cortex and the STN; DBS decreased more often the STN beta power than cortical beta power.

In MEG recording with DBS on the mu rhythm amplitude correlated significantly with the UPDRS rigidity scores. Consequently, mu rhythm modifications by DBS seem to be related to the therapeutic effect of DBS. DBS may also reduce pathological, rigidity-related oscillations or "noise" in the spontaneous activity in the sensorimotor system. When DBS was off, however, the source strengths of beta band activity did not correlate with UPDRS rigidity subscores. It has also been reported that total power of the signal recorded by the STN electrodes in the 13 – 35 Hz range did not correlate with the clinical state at rest without treatment (Chen et al., 2010).

The 6 – 10 Hz signal from both the pericentral and occipital areas correlated with the action tremor when DBS was off. Although the patients were resting during the measurements, a slight action tremor in the 7 – 12 Hz range could not be excluded.

In PD patients without DBS, the EEG and MEG resting state oscillatory activities slow down (Soikkeli et al., 1991; Bosboom et al., 2006). The average peak frequency of the spontaneous oscillatory activity across the whole cortex has also been shown to be lower when stimulation was off than when it was on (Cao, 2015). In our study DBS did not modify the peak frequencies of the oscillatory activity. Nevertheless, the occipital alpha peak frequency correlated negatively with total UPDRS motor and rigidity subscores, which indicated that the motor condition was worse when occipital alpha frequency was lower.

The number of patients in this study was quite small for calculating correlations and correlation does not necessarily imply causality.

5.4 The effects of DBS on CMC (Study III)

Significant coherence peaks were detected in the 13 – 25 Hz range in 15 out of 19 patients. The mean frequency was 17.7 (± 3.2) Hz when DBS was on and 18.1 (± 3.1) Hz when DBS was off. 11 patients had statistically significant CMC for both DBS on and off conditions. Two patients had a significant coherence only when DBS was on and two patients had CMC only when DBS off (Figure 10).

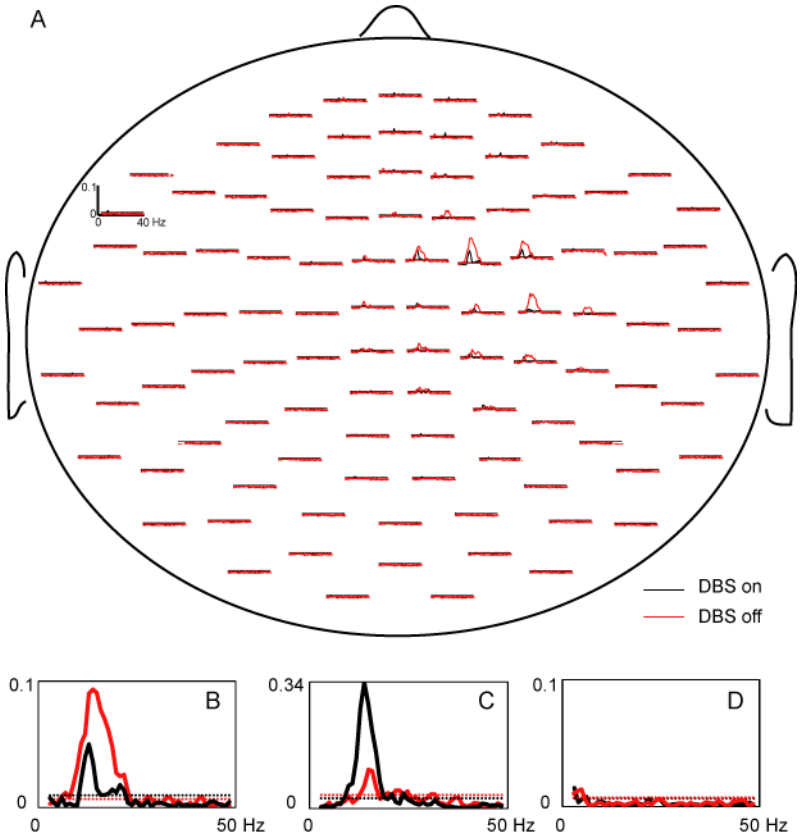

Figure 10. A: Cortico-muscular coherence spectra of one patient from 102 gradiometer pairs. The sensors are viewed from above, and the patient's nose points upwards. The maximum CMC peaks over the sensorimotor cortex contralateral to the activated hand. B-D: CMC from one sensor over contralateral sensorimotor cortex from one patient showing a decrease in CMC when the DBS was on (B), one patient showing an increase in CMC when the DBS was on (C) and one patient without CMC (D). The black line depicts DBS on, the red line shows DBS off. Dotted horizontal lines indicate the 99%-significance level. Modified from Study III.

Eight patients had a significant CMC both when DBS was on and off in the 6 – 13 Hz range; the mean frequency was 10.8 (± 2.0) DBS on and 11.1 (± 1.9) when DBS off. Moreover, three patients had CMC only when DBS was on and three patients only when DBS was off in this frequency range, and four patients did not manifest CMC when DBS was either on or off. CMC in the 4 – 6 Hz range was found only in five patients. The CMC peak frequencies or strengths did not differ significantly between DBS on and off.

5.4.1 Correlation of CMC with the motor state

The CMC peak amplitude in the 13 – 25 Hz range correlated negatively with tremor scores when DBS was off (r_s = -0.561, n = 13, p = 0.046, two-tailed); when tremor scores were high the CMC peak amplitudes were small. In the 6 – 13 Hz range the CMC peak amplitudes correlated negatively with the tremor scores of the activated hand when DBS was off (r_s = -0.616, n = 12, p = 0.033, two-tailed).

When DBS was on, the CMC amplitude in the 13 – 25 Hz range correlated negatively with the tremor of the activated arm (r_s = -0.756, n = 10, p = 0.011, two-tailed) and total tremor scores (r_s = -0.795, n = 10, p = 0.006, two-tailed). The CMC peak frequency and the tremor scores of the activated hand correlated negatively when DBS on (r_s = -0.654, n = 10, p = 0.040, two-tailed) in the 6 – 13 Hz band.

In the patients whom UPDRS scores were decreased more than 30% by DBS, correlations between CMC parameters and tremor scores were present as well. Peak frequency in the 6 – 13 Hz band correlated negatively with total tremor scores when DBS was on (r_s = -0.836, n = 6, p = 0.038, two-tailed). Moreover, CMC peak amplitude and the rigidity scores of the activated hand correlated negatively when the DBS was on in the 13 – 25 Hz band (r_s = -0.769, n = 8, p = 0.026, two-tailed) in this group.

5.4.2 CMC correlation with clinical conditions of patients

The CMC peak amplitude in the 6 – 13 Hz band correlated with age of the patients when DBS was off (r_s = 0.599, n = 12, p = 0.040, two-tailed). In

patients for whom the DBS decreased the UPDRS scores by more than 30%, age correlated with the peak frequency when DBS was off (r_s = 0.845, n = 6, p = 0.034, two-tailed) and with the peak amplitude when DBS was on (r_s = 0.812, n = 6, p = 0.05, two-tailed).

5.4.3 Differences between subgroups based on the presence of CMC in the 13 – 25 Hz band

The patients were divided into three subgroups with different CMC appearance: One group had no CMC for the DBS on or off conditions (CMC- subgroup), another group had CMC in only DBS on or off (CMC± subgroup) and CMC+ subgroup had CMC both DBS on and off.

All patients that had CMC in the 13 – 25 Hz band for DBS on and off conditions (CMC+ subgroup) had a rigid-akinetic type of PD. DBS voltages differed between the groups: the largest stimulation voltages were given to the CMC+ subgroup (p = 0.05). The patients in the CMC± subgroup managed with the lowest LEDD (p = 0.015). There was no difference in the preoperative LEDD between the subgroups. The mean time between the DBS operation and the MEG measurement differed between the groups (p = 0.013). The age or disease duration did not differ significantly between these subgroups. The total UPDRS motor scores between these subgroups were statistically different (DBS on p = 0.028; DBS off: p = 0.020). The best UPDRS scores were obtained from the CMC+ subgroup both for DBS on and off conditions. (Table 3)

Table 3. Clinical parameters in different subgroups based on the presence of CMC in the 13 – 25 Hz band. CMC+ = CMC both DBS on and off, CMC- = no CMC for DBS on or off, CMC± = CMC DBS on or off, LEDD = levodopa equivalent daily dose

	CMC+	CMC-	CMC±
DBS voltages	3.5 ± 0.9 V	2.7 ± 0.6 V	2.6 ±0.3 V
LEDD	1070 ± 420 mg	1410 ± 655mg	440 ± 160 mg
Time between DBS operation and MEG measurement	10 ± 7.3 months	23 ± 3.9 months	5.5 ± 0.9 months
Total UPDRS, DBS on	16.5 ± 6.0	31.3 ± 6.7	24.5 ± 15.6
Total UPDRS, DBS off	28.2 ± 12.9	39.3 ± 9.1	55.8 ± 16.7

5.4.4 Discussion of Study III

CMC was found in this patient group as frequently as that reported for healthy subjects (e.g. (Pohja et al., 2005; Bourguignon et al., 2013)). The DBS effect on CMC varied between individuals. We did not find systematic increases in CMC in the 13 – 25 Hz range, contrary to our anticipated increase of CMC with DBS, based on a previous PD study reporting an increase in CMC by levodopa (Salenius et al., 2002). The functional role of CMC even in healthy subjects is not yet fully understood. CMC may be missing in people with totally normal ability to move and training has shown to have conflicting effects on it (Ushiyama et al., 2010; Mendez-Balbuena et al., 2012).

CMC in patients with an early stage PD did not differ from age-matched controls (Pollok et al., 2012); thus a weak CMC is probably not a hallmark of PD. The effect of levodopa on CMC also varies between patients (Salenius et al., 2002). Enhancement of CMC activity by levodopa was also not detected in recordings one day after DBS electrode implantation (Hirschmann et al., 2013).

It is also possible that STN stimulation suppresses cortical activity in such a small area close to the hyperdirect pathway (Whitmer et al., 2012) that CMC is not influenced by such focal changes. STN-DBS may also modulate the motor function by altering the descending outputs from the basal ganglia, e.g., via the brainstem motor control centers (Delwaide et al., 2000).

The negative correlation of CMC in the 13 – 25 band with UPDRS tremor subscores may demonstrate the well-known suppression of the CMC by movements (such as tremor) in this frequency range. An increase in CMC with DBS treatment was reported to correlate with decreased tremor in three patients (Park et al., 2009).

Some features of our data, however, indicate the beneficial effect of CMC in the 13 – 25 Hz band. The best UPDRS scores were seen in patients who manifested CMC in this frequency band for DBS in both on and off conditions. Moreover, the patients with no CMC over this range needed the most medication.

CMC may reflect both the functional properties of muscle co-ordination and some pathophysiological features of PD such as rigidity. Transcranial alternating current stimulation (tACS) at 20 Hz increased beta CMC and slowed down movements in healthy control subjects (Pogosyan et al., 2009), whereas in PD patients it attenuated CMC and made the amplitude of finger tapping more regular (Krause et al., 2014). We were not able to separate the functional and pathological features of CMC.

CMC peak amplitude and frequency both correlated negatively with UPDRS tremor scores in the 6 – 13 Hz range. The importance of this finding remains uncertain because several patients had zero tremor scores.

5.5 CMC and CKC in 10 healthy volunteers (Study IV)

Significant CMC was detected in 19 out of 20 hemispheres, and significant CKC was found in 20 hemispheres of 10 healthy subjects. Data from 19 hemispheres with both CMC and CKC were analyzed. The frequency distributions of the CMC and CKC peaks overlapped at least in part in 15 hemispheres. The similarities of the CKC and CMC values in both hemispheres enabled their pooling across the hemispheres. The intraindividual variability between the right and left hemispheres within a subject was less prominent than the noticeable variability seen when CMC and CKC were compared between individuals.

The mean peak CMC frequency was 23 Hz and CKC mean peak frequency 21 Hz ($p = 0.013$). The mean peak frequencies of CMC and CKC correlated ($r_s = 0.681$, $n = 19$, $p = 0.001$, two tailed). The mean maximum CMC amplitude was 0.1 ± 0.05 and the mean maximum CKC amplitude was 0.08 ± 0.04 ($p = 0.059$). Maximum CMC and maximum CKC amplitudes correlated significantly ($r_s = 0.575$, $n = 19$, $p = 0.010$, two tailed). The source location co-ordinates did not differ significantly between CMC and CKC within different hemispheres (Figure 11).

The peak frequency of accelerometer power spectrum between 6 – 14 Hz, considered to contain the tremor frequency, did not correlate with CMC ($r_s = -0.178$, $n = 19$, $p = 0.465$, two tailed) or CKC ($r_s = 0.045$, $N = 19$, $p = 0.854$, two tailed) peak frequencies.

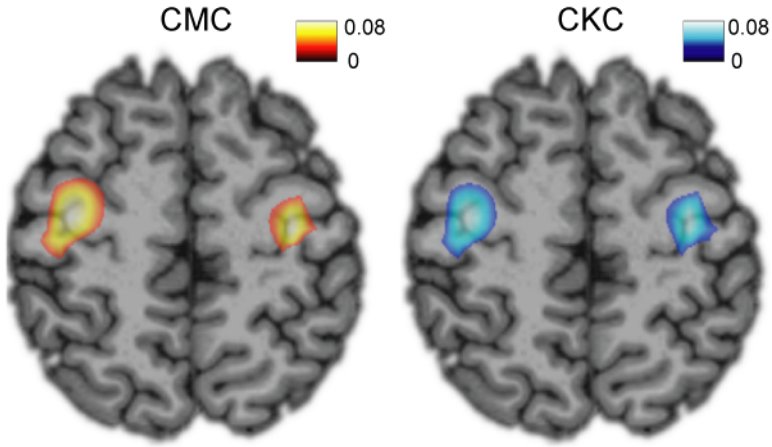

Figure 11. Source localization of CMC (left) and CKC (right) in one subject. Modified from Study IV.

5.5.1 Discussion of Study IV

CMC and CKC spectra in most subjects resemble each other and the beamformer source locations of simultaneously recorded CMC and CKC were nearly identical. The task was to extend the wrist and hold the hand still, thus the accelerometer signals (and CKC) were generated by postural tremor. The accelerometer power spectra revealed a low-frequency peak between 5 and 11 Hz in nine out of ten patients. This peak probably has it origins in the small-amplitude postural tremor. Hence, we suggest that the physiological mechanisms related to postural tremor are registered in CMC. A previous study of PD patients revealed an elevated CMC in the 12 – 18 Hz band in patients with strong postural tremor (Caviness et al., 2006) supporting this notion.

Small differences between CMC and CKC spectra are not surprising even when they reflect the same phenomenon, because the EMG electrode records signals from one muscle but the postural tremor probably relates to activity of several muscles.

The accelerometer signals are also useful in CKC estimates in the stationary hand position used in this study. The accelerometer is often easier to use than EMG as EMG electrode placement is more vulnerable and when the EMG electrode is attached on the skin the skin may move relative to the examined muscle.

6. ADDITIONAL MATERIAL

6.1 Motivation

The motivation for this additional previously unpublished material came from the numerous sharp peaks found in the spectra of spontaneous brain activity during DBS treatment (Study II, Figure 5). The peak frequencies were so regular in the patients that their biological origin was doubtful. Nevertheless, the patients were stimulated by regular pulse frequencies; therefore it could have been possible that this exogenous rhythm paced the neurons in a very regular way.

6.2 Methods

We explored this phenomenon in more detail by measuring the pure DBS signal without the 'disturbing' neural activity and by taking the measurements in such a way as to test several different stimulator parameters without concerns. Watermelons turned out to be suitable 'phantom brains'.

We implanted Kinetra and Activa PC Neurostimulators into watermelons. The melon measurements were carried out at the BioMag Laboratory and at MEG Core of the Brain Research Unit, Aalto University. The MEG centers at Aalto University and the Helsinki University have Elekta Vectorview™ MEG devices but their software are slightly different. The MEG at Aalto University enables recordings with higher sampling rates.

One-minute recordings were collected for different DBS and MEG parameters (Figure 12). The spectra were calculated with Graph software (Elekta Oy) with 50% overlapping 1024-point Hanning windows. No statistical comparisons were done.

Figure 12. DBS programming between watermelon recordings

6.4. Results

Similar spectral peaks as found in patient data (Study II) were detected in the watermelon measurements during DBS. This indicates that their generation did not require a neural substrate, and they were consequently stimulation artifacts.

tSSS method was also efficient at suppressing DBS artifacts from these data (Figure 13 A). The spectral peak frequencies were slightly different between Kinetra and Activa PC DBS devices (Figure 13 B). Different MEG settings (band pass, sampling frequency) modified the peak frequencies (Figure 13 C). As the higher sampling frequency generated artifacts at the lower frequencies than lower sampling frequencies, the artifacts are not totally explained by an aliased DBS-interference component.

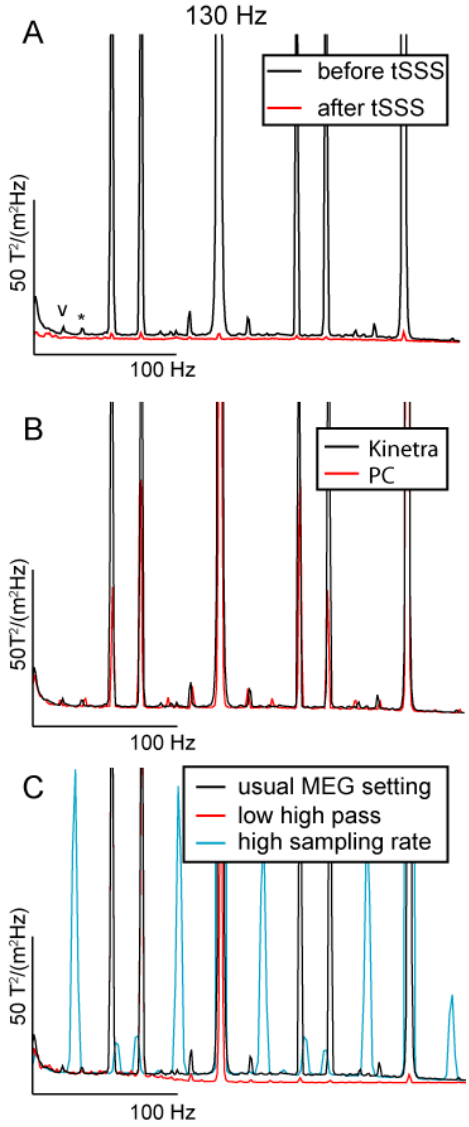

Figure 13. The amplitude spectra of DBS-induced spectral peaks in a watermelon measured in the BioMag laboratory. The frequency range is 0 – 300 Hz.
A: The amplitude spectra before (black) and after (red) tSSS. Artifact peaks similar to those found in patient measurements were detected (peak at 20.9 Hz marked with "v" and at 33.9 Hz with "*"). B: Comparison between Kinetra (black) and Activa PC (red) devices. Small differences were observed in amplitudes and frequencies of spectral peaks. C: The used band pass and sampling frequency had an effect on artifact peaks. The black line represents the usual settings (bandpass 0.03 – 330 Hz, sampling frequency 1011 Hz). When the high pass filter was set at 100 Hz the artifact peaks decreased but did not totally vanish (red). Higher sampling rate at 2018 Hz (turquoise) increased the peaks and changed their frequencies.

6.5 Discussion of additional material

These DBS measurements with watermelons confirmed that the sharp spectral peaks seen in our patient data are mostly artifacts. This finding does not rule out that some neural activity could be driven by the DBS stimulation frequency (see e.g. Walker et al., 2012). The experiments in Study IV also verified that the MEG recording parameters also have an effect on the appearance of the artifactual frequency peaks, which highlights the importance of parameter optimization. The artifact patterns also differed between the two MEG devices (not shown) so that the artifact problems of different MEG centers may not be identical.

7. GENERAL DISCUSSION

The effects of STN-DBS on the brain's electrical activity were studied in advanced PD patients treated with DBS. The measurements included recordings of evoked potentials, spontaneous brain activity and CMC. All were measured when DBS was both on and off. One study (IV) was done with healthy volunteers to examine the effect of postural tremor on CMC to gain a better understanding of the properties of CMC.

The tSSS method suppressed the DBS-induced magnetic artifacts quite well. Nevertheless all artifacts were not totally erased. Therefore the data must be examined carefully even after using artifact suppression with tSSS. Reducing the correlation limit of tSSS enhanced the clearance of the data but at some point the brain signals may be affected as well. The correlation limit of 0.8 has been shown to be fairly safe (Medvedovsky et al., 2009). The artifact problems, related to the placement of the DBS wires and battery and filter settings, should be taken into account during the study design. The frequencies used by head indicator coils and the sampling rates that are optimal for DBS recordings should both be selected carefully.

These studies focused on signals at and below the beta range. We observed that the DBS-related artifacts centered on frequencies above this range. The artifacts of DBS may be particularly hard to cope with when exploring signals in higher frequency bands. For example, DBS may also induce brain activity in the gamma band frequencies (Garcia et al., 2005). Oscillations at about 300-Hz have been shown to be of interest in PD because LFP recordings of STN have indicated 300-Hz rhythm that is dopamine- and movement-dependent (Foffani et al., 2003). At present, oscillations at 300-Hz frequency range are not easily studied by MEG in patients with DBS on.

The effects of DBS on cortical activity were studied in this thesis. The results were somewhat inconsistent. We did not find a simple parameter that exclusively reflected the effect of STN-DBS in advanced PD. Although several studies emphasize the importance of cortical activity in directing STN activity in animals (Gradinaru et al., 2009) and in patients (Marsden et al., 2001; Fogelson et al., 2006; Litvak et al., 2011), some effects of DBS may be mediated via deeper brain structures that are not

directly visualized in MEG signals (Delwaide et al., 2000). It may also be the case that the DBS-induced effects are better highlighted in more complex aspects of cortical electrophysiology, not analyzed by us, e.g. in reduced cortical phase-amplitude relationships (de Hemptinne et al., 2015).

The patients could have had occasional tremor periods during the recordings, which might have affected the spectra of spontaneous brain activity (Mäkelä et al., 1993) or CMC. A slight tremor may affect the CMC results by generating a CMC at the tremor frequency and its harmonics (Volkmann et al., 1996; Timmermann et al., 2003). A strong tremor might even induce widespread fluctuations of the measured magnetic fields. If CMC is affected by postural tremor as we speculate, then the monitoring the tremor during the measurement with accelerometer would be relevant.

Antiparkinsonian medication could also produce some variability in our results. The patients continued their medication during the recordings to make the measurement easier for them. Therefore, we reported combined effects of DBS and antiparkinsonian medication. This may have had an influence on the results. A saturation effect was not probable in our studies as the DBS improved the motor state of the patients. Although medication was administered during the measurements, the fluctuations in the medication levels could not be totally controlled.

The stun effect, improvement of the symptoms by the micro-lesion caused by electrode insertion, should not have been problem in our studies as it has reported to vanish within one month after insertion of the electrodes (Jech et al., 2012). We did not have a precise delineation of the electrode locations in the STN at our disposal. However, the DBS was efficient in all our patients. This indicated that the DBS target was adequate.

The CMC has traditionally been estimated between EMG and brain signals. However, EMG has many limitations. Even the exact EMG-electrode placement may be difficult if the skin moves in relation to the underlying muscles during or between the recordings. The usefulness of EMG rectification has also been debated lately. Previously it has been regularly used in CMC calculations. Rectification of EMG was thought to enhance firing rate information and thus be a necessary pre-processing step for CMC analysis (Myers et al., 2003). The EMG was rectified in Study III. Recent literature has argued against the rectification of EMG

(Neto and Christou, 2010; McClelland et al., 2012). Therefore the EMG rectification was omitted in Study IV. The rectification has been reported to have erratic effects on the coherence spectra and even obscure the CMC detection in some cases (McClelland et al., 2012), thus it may have affected our results in Study III unfavourably. The problems regarding EMG in such studies make alternative approaches interesting and data in Study IV indicates that an accelerometer may also be used for coherence estimations during stationary hand positions, and not only during the movements.

At least three hours of STN-DBS off is required to establish a steady DBS off state for efficacy studies (Temperli et al., 2003). However, about 50% of the total change has been estimated to occur in as little as 5 minutes after DBS is turned off (Little et al., 2013). In all but one of our patients the MEG measurements were done first with DBS on and then DBS off. The DBS switching was done in a shielded room but the patient, seated in the measurement chair, was taken out from the helmet to get some distance between the MEG sensors and programmer device. There was an interval of several minutes before measurements were resumed. The actual time of switching off DBS before the DBS off measurements was not recorded. Most often the DBS off measurements were started with evoked field recordings, which thus had the least time to be affected by turning DBS off. The difference in results between DBS on and off states could have been clearer if the time between switching off the DBS and starting the measurement had been longer.

There are only a few previous MEG studies of chronically DBS treated PD patients, and those studies used small groups of patients. We, by comparison, studied a relatively large number of patients. Nevertheless, the patient numbers are still small, particularly for subgroup analyses, and this needs to be taken into account when interpreting the statistical results.

In the future, DBS that is adaptive to the clinical condition of individual patients may produce better efficacy and longer duration of the implanted battery than the present stimulation strategies. Studies of adaptive DBS in Parkinsonian non-human primates (Rosin et al., 2011) and in patients (Little et al., 2013) have suggested a potentially better efficacy in ameliorating PD symptoms than conventional DBS. The adaptability can be obtained by monitoring the electrophysiological changes of the patient. MEG may provide clues for the appropriate neuromodulatory effects of

DBS on long-range brain networks of PD patients, which would be a prerequisite for an optimal clinical outcome.

8. SUMMARY

MEG studies of DBS patients are challenging. DBS may preclude MEG measurements totally as artifacts produced by DBS conceal brain signals in the recorded data. The studies presented and summarised in this thesis show that the MEG data recorded in DBS-treated PD patients is amenable to analyses in the vast majority of the cases after artifact rejection by tSSS. Studies of previously well known SEFs and AEFs demonstrate that DBS artifacts can be removed efficiently and that the remaining signals contain physiologically valid data (Study I).

The precise mechanisms of action of the DBS treatment are still unclear. Thus we studied the alterations in the electrical activity of the brain caused by DBS. The auditory and somatosensory evoked fields in Study I revealed an AEF N100m amplitude increase in the right hemisphere for ipsilateral sound stimuli when the DBS was on. This indicated that cortical activity is modified by DBS.

The effects of DBS on spontaneous brain activity and CMC were not uniform between patients. Nonetheless, some correlations to clinical parameters were found. Patients with a clear suppression of beta range source strength of sensorimotor spontaneous activity also had the clearest reduction in rigidity (Study II). Levodopa has been reported to enhance CMC in some studies, but we did not find a similar systematic increase in CMC in the 13 – 25 Hz band during DBS in Study III. In contrast, CMC decreased in the majority of the patients during DBS. However, the absence of CMC was associated with higher doses of medication. This suggested that CMC may partly reflect compensatory phenomena to diminished dopamine demand (Study III).

CMC may reflect the interplay between cortical and muscle activities. However, the functional role of CMC even in healthy subjects is not yet fully understood. We studied simultaneous CMC and CKC of healthy volunteers during a static hold task to enhance our knowledge of the physiology of CMC. CMC and CKC were quite similar in healthy volunteers. This suggests that CMC may relate to postural tremor, the source of kinematics in the static muscle contraction task (Study IV). It was possible to measure CKC during the static wrist extension in healthy

subjects. Thus an accelerometer may prove to be useful for coherence measurements in the future.

Data in this thesis show that MEG studies of DBS-treated PD patients are feasible after applying tSSS for artifact suppression. DBS modifies cortical electrical activity, and some of these modifications correlate with the clinical improvement of PD patients. Moreover, the accelerometer signals are useful in CKC estimates recorded during a stationary hand position task.

DBS is also used as an experimental therapy in several other disorders, such as epilepsy, obsessive-compulsive disorders, dementia and chronic pain, therefore the methods used in this thesis can be applied to study the pathophysiology of these conditions as well.

ACKNOWLEDGEMENTS

This thesis project was carried out in the BioMag Laboratory and in the Department of Neurology of Helsinki University Hospital. I want to express my gratitude for BioMag Laboratory for providing research facilities. Docent Markus Färkkilä and Docent Nina Forss the former and present heads of the Department of Neurology and Professor Timo Erkinjuntti are particularly thanked for providing an inspiring and research-friendly working atmosphere.

My heartfelt thanks go to my supervisors Docent Eero Pekkonen and Docent Jyrki Mäkelä. Eero introduced me to DBS and taught me a lot about Parkinson's disease. Without him the recruitment of the patients to these studies would have been impossible. Jyrki led me to the world of MEG. His wide experience has been crucial in meeting the challenges during this project. I feel privileged to have had two so easily approachable and dedicated supervisors.

I want thank Docent Valtteri Kaasinen and Professor Esa Mervaala for carefully reviewing the manuscript and giving valuable comments. My sincere thanks also go to Professor Karen Østergaard for accepting the role of opponent.

I am deeply grateful for all my co-authors. Special thanks to Samu Taulu, without tSSS this project would never have started, and Jussi Nurminen and Jarkko Luoma who both patiently helped me with computers and answered all my small and big questions related to physics and to MEG analyses.

Without the great “BioMag people” this work might not have seen the end. No matter how difficult the problems with this project were, you were a good reason to come to the BioMag Laboratory. Thanks to all of you, Ville, Andrey, Bei, Päivi, Juha M, Juha H, Juha W, Simo, Selja, Pantelis, Ritva, Niko, Tuuli, Eini and others.

Thank you also goes to Veikko Jousmäki for the accelerometer device and Lauri Parkkonen for helping with the water-melon measurements in Aalto University.

I want also thank Erik Johansen and Markus Butz for many interesting discussions, also about MEG.

My sincere thanks to my colleagues and friends in the Department of Neurology in Meilahti. Especially my thanks to Docent Nina Forss and Docent Seppo Kaakkola for being my follow-up group as well as Jukka Lyytinen for helping me with the DBS tunings when needed. Kristina and Eeva, you have been important peer supports, which I highly appreciate. My warmest thanks to my colleagues in Peijas Hospital Pia, Marjo, Marja, Krista and Chief of Neurology Department in Peijas Hospital Elena Haapaniemi who has been flexible with timetables and gave her support to this project.

I am grateful to Pirjo Kari and Marja Bigler for helping me with all the practical issues. Study nurses Suvi Heikkilä and Jari Kainulainen have been great with the patients and patient with me, thanks for that.

I am thankful to the patients for participation and giving their time for the sake of science.

I give my most warm thanks to my parents Kirsti and Timo and my sister Maria and her family for supporting and believing in me.
Finally, I want to thank Mikko, you have been the most important motive for me to finish this project. Thank you for diverting my attention outside MEG and Parkinson's disease when needed.

This project was financially supported by the Academy of Finland (Grant No. 122725) and by the SalWe Research Program for Mind and Body (Tekes – the Finnish Funding Agency for Technology and Innovation grant 1104/10). My work was also financially supported by the Finnish Parkinson Foundation, the Finnish Brain Foundation and the Finnish Medical Foundation.

Helsinki, October 2015

Katja Airaksinen

REFERENCES

Abelson JL, Curtis GC, Sagher O, Albucher RC, Harrigan M, Taylor SF, Martis B, Giordani B. Deep brain stimulation for refractory obsessive-compulsive disorder. *Biol Psychiatry* 57: 510–516, 2005.

Albin RL, Young AB, Penney JB. The functional anatomy of basal ganglia disorders. *Trends Neurosci* 12: 366–375, 1989.

Alves G, Forsaa EB, Pedersen KF, Gjerstad MD, Larsen JP. Epidemiology of Parkinson's disease. *J Neurol* 255: 18–32, 2008.

Baillet S. The Dowser in the Fields: Searching for MEG Sources. In: Hansen P, Kringelbach M, Salmelin R. *MEG: An Introduction to Methods*. Oxford University Press, 2010 p.83–123.

Benabid AL, Chabardes S, Mitrofanis J, Pollak P. Deep brain stimulation of the subthalamic nucleus for the treatment of Parkinson's disease. *Lancet Neurol* 8: 67–81, 2009.

Benabid AL, Pollak P, Louveau A, Henry S, de Rougemont J. Combined (Thalamotomy and Stimulation) Stereotactic Surgery of the VIM Thalamic Nucleus for Bilateral Parkinson Disease. *Stereotact Funct Neurosurg* 50: 344–346, 1987.

Bosboom JLW, Stoffers D, Stam CJ, van Dijk BW, Verbunt J, Berendse HW, Wolters EC. Resting state oscillatory brain dynamics in Parkinson's disease: An MEG study. *Clin Neurophysiol* 117: 2521–2531, 2006.

Bourguignon M, Jousmäki V, Marty B, Wens V, Op de Beeck M, Van Bogaert P, Nouali M, Metens T, Lubicz B, Lefranc F, Bruneau M, De Witte O, Goldman S, De Tiège X. Comprehensive functional mapping scheme for non-invasive primary sensorimotor cortex mapping. *Brain Topogr* 26: 511–523, 2013.

Bourguignon M, De Tiège X, de Beeck MO, Pirotte B, Van Bogaert P, Goldman S, Hari R, Jousmäki V. Functional motor-cortex mapping using corticokinematic coherence. *NeuroImage* 55: 1475–1479, 2011.

Boyle A, Ondo W. Role of Apomorphine in the Treatment of Parkinson's Disease. *CNS Drugs* 29: 83–89, 2015.

Bronstein JM, Tagliati M, Alterman RL, Lozano AM, Volkmann J, Stefani A, Horak FB, Okun MS, Foote KD, Krack P, Pahwa R, Henderson JM, Hariz MI, Bakay RA, Rezai A, Marks WJ, Moro E, Vitek JL, Weaver FM, Gross RE, DeLong MR. Deep brain stimulation for Parkinson disease: an expert consensus and review of key issues. *Arch Neurol* 68: 165, 2011.

Bronte-Stewart H, Barberini C, Koop MM, Hill BC, Henderson JM, Wingeier B. The STN beta-band profile in Parkinson's disease is stationary and shows prolonged attenuation after deep brain stimulation. *Exp Neurol* 215: 20–28, 2009.

Brown P. Muscle sounds in Parkinson's disease. *The Lancet* 349: 533–535, 1997.

Brown P, Oliviero A, Mazzone P, Insola A, Tonali P, Lazzaro VD. Dopamine Dependency of Oscillations between Subthalamic Nucleus and Pallidum in Parkinson's Disease. *J Neurosci* 21: 1033–1038, 2001.

Brown P, Salenius S, Rothwell JC, Hari R. Cortical correlate of the Piper rhythm in humans. *J Neurophysiol* 80: 2911–2917, 1998.

Burn DJ, Rowan EN, Allan LM, Molloy S, O'Brien JT, McKeith IG. Motor subtype and cognitive decline in Parkinson's disease, Parkinson's disease with dementia, and dementia with Lewy bodies. *J Neurol Neurosurg Psychiatry* 77: 585–589, 2006.

Cao C, Li, Dianyou, Jiang, Tianxiao, Ince, Nuri Firat, Zhan, Shikun, Zhang, Jing, Sha, Zhiyi, Sun, Bomin. Resting state cortical oscillations of PD patients without and with Subthalamic deep brain stimulation, a MEG study. *J. Clin. Neurophysiol 32:109*–118, 2015.

Carlsson A. Treatment of Parkinson's with L-DOPA. The early discovery phase, and a comment on current problems. *J Neural Transm* 109: 777–787, 2002.

Caviness JN, Shill HA, Sabbagh MN, Evidente VGH, Hernandez JL, Adler CH. Corticomuscular coherence is increased in the small postural tremor of Parkinson's disease. *Mov Disord* 21: 492–499, 2006.

Chen CC, Hsu YT, Chan HL, Chiou SM, Tu PH, Lee ST, Tsai CH, Lu CS, Brown P. Complexity of subthalamic 13–35 Hz oscillatory activity directly correlates with clinical impairment in patients with Parkinson's disease. *Exp Neurol* 224: 234–240, 2010.

Connolly AT, Bajwa JA, Johnson MD. Cortical magnetoencephalography of deep brain stimulation for the treatment of postural tremor. *Brain Stimulat* 5: 616–624, 2012.

Connolly BS, Lang AE. Pharmacological treatment of parkinson disease: A review. *JAMA* 311: 1670–1683, 2014.

Conway BA, Halliday DM, Farmer SF, Shahani U, Maas P, Weir AI, Rosenberg JR. Synchronization between motor cortex and spinal motoneuronal pool during the performance of a maintained motor task in man. *J Physiol* 489: 917–924, 1995.

DeLong MR. Primate models of movement disorders of basal ganglia origin. *Trends Neurosci* 13: 281–285, 1990.

DeLong MR. The Basal Gaglia. In: Kandel E, Schwartz J, Jessell T**.** *Principles of Neural Science, Fourth Edition*. McGraw-Hill Companies,Incorporated, 2000. p. 853–867.

Delwaide PJ, Pepin J-L, Pasqua VD, Noordhout AM de. Projections from basal ganglia to tegmentum: a subcortical route for explaining the pathophysiology of Parkinson's disease signs? *J Neurol* 247: II75–II81, 2000.

Deuschl G, Schade-Brittinger C, Krack P, Volkmann J, Schäfer H, Bötzel K, Daniels C, Deutschländer A, Dillmann U, Eisner W, Gruber D, Hamel W, Herzog J, Hilker R, Klebe S, Kloss M, Koy J, Krause M, Kupsch A, Lorenz D, Lorenzl S, Mehdorn HM, Moringlane JR, Oertel W, Pinsker MO, Reichmann H, Reuss A, Schneider G-H, Schnitzler A, Steude U, Sturm V, Timmermann L, Tronnier V, Trottenberg T, Wojtecki L, Wolf E, Poewe W, Voges J, German Parkinson Study Group, Neurostimulation Section. A randomized trial of deep-brain stimulation for Parkinson's disease. *N Engl J Med* 355: 896–908, 2006.

Drory VE, Inzelberg R, Groozman GB, Korczyn AD. N30 somatosensory evoked potentials in patients with unilateral Parkinson's disease. *Acta Neurol Scand* 97: 73–76, 1998.

Eggers C, Pedrosa DJ, Kahraman D, Maier F, Lewis CJ, Fink GR, Schmidt M, Timmermann L. Parkinson Subtypes Progress Differently in Clinical Course and Imaging Pattern. *PLoS ONE* 7: e46813, 2012.

Elberling C, Bak C, Kofoed B, Lebech J, Saermark K. Auditory magnetic fields from the human cerebral cortex: location and strength of an equivalent current dipole. *Acta Neurol Scand* 65: 553–569, 1982.

Eusebio A. Deep brain stimulation can suppress pathological synchronisation in parkinsonian patients. *J Neurol Neurosurg Psychiatry* 82: 569–573, 2011.

Eusebio A, Cagnan H, Brown P. Does suppression of oscillatory synchronisation mediate some of the therapeutic effects of DBS in patients with Parkinson's disease? *Front Integr Neurosci* 6: 47, 2012.

Fenoy AJ, Simpson RK. Management of device-related wound complications in deep brain stimulation surgery. *J Neurosurg* 116: 1324–1332, 2012.

Ferreira JJ, Katzenschlager R, Bloem BR, Bonuccelli U, Burn D, Deuschl G, Dietrichs E, Fabbrini G, Friedman A, Kanovsky P, Kostic V, Nieuwboer A, Odin P, Poewe W, Rascol O, Sampaio C, Schüpbach M, Tolosa E, Trenkwalder C, Schapira A, Berardelli A, Oertel WH. Summary of the recommendations of the EFNS/MDS-ES review on therapeutic management of Parkinson's disease. *Eur J Neurol* 20: 5–15, 2013.

Fisher R, Salanova V, Witt T, Worth R, Henry T, Gross R, Oommen K, Osorio I, Nazzaro J, Labar D, Kaplitt M, Sperling M, Sandok E, Neal J, Handforth A, Stern J, DeSalles A, Chung S, Shetter A, Bergen D, Bakay R, Henderson J, French J, Baltuch G, Rosenfeld W, Youkilis A, Marks W, Garcia P, Barbaro N, Fountain N, Bazil C, Goodman R, McKhann G, Babu Krishnamurthy K, Papavassiliou S, Epstein C, Pollard J, Tonder L, Grebin J, Coffey R, Graves N, the SANTE Study Group. Electrical stimulation of the anterior nucleus of thalamus for treatment of refractory epilepsy. *Epilepsia* 51: 899–908, 2010.

Foffani G, Priori A, Egidi M, Rampini P, Tamma F, Caputo E, Moxon KA, Cerutti S, Barbieri S. 300- Hz subthalamic oscillations in Parkinson's disease. *Brain* 126: 2153–2163, 2003.

Fogelson N, Kühn AA, Silberstein P, Limousin PD, Hariz M, Trottenberg T, Kupsch A, Brown P. Frequency dependent effects of subthalamic nucleus stimulation in Parkinson's disease. *Neurosci Lett* 382: 5–9, 2005.

Fogelson N, Williams D, Tijssen M, Bruggen G van, Speelman H, Brown P. Different Functional Loops between Cerebral Cortex and the Subthalmic Area in Parkinson's Disease. *Cereb Cortex* 16: 64–75, 2006.

Follett KA, Torres-Russotto D. Deep brain stimulation of globus pallidus interna, subthalamic nucleus, and pedunculopontine nucleus for Parkinson's disease: which target? *Parkinsonism Relat Disord* 18 Suppl 1: S165–167, 2012.

Follett KA, Weaver FM, Stern M, Hur K, Harris CL, Luo P, Marks WJ, Rothlind J, Sagher O, Moy C, Pahwa R, Burchiel K, Hogarth P, Lai EC, Duda JE, Holloway K, Samii A, Horn S, Bronstein JM, Stoner G, Starr PA, Simpson R, Baltuch G, De Salles A, Huang GD, Reda DJ. Pallidal versus Subthalamic Deep-Brain Stimulation for Parkinson's Disease. *N Engl J Med* 362: 2077–2091, 2010.

Forss N, Hari R, Salmelin R, Ahonen A, Hämäläinen M, Kajola M, Knuutila J, Simola J. Activation of the human posterior parietal cortex by median nerve stimulation. *Exp Brain Res* 99: 309–315, 1994a.

Forss N, Salmelin R, Hari R. Comparison of somatosensory evoked fields to airpuff and electric stimuli. *Electroencephalogr Clin Neurophysiol* 92: 510–517, 1994b.

Garcia L, Audin J, D'Alessandro G, Bioulac B, Hammond C. Dual Effect of High-Frequency Stimulation on Subthalamic Neuron Activity. *J Neurosci* 23: 8743–8751, 2003.

Garcia L, D'Alessandro G, Bioulac B, Hammond C. High-frequency stimulation in Parkinson's disease: more or less? *Trends Neurosci* 28: 209–216, 2005.

Garcia PA, Aminoff MJ, Goodin DS. The frontal N30 component of the median- derived SEP in patients with predominantly unilateral Parkinson's disease. *Neurology* 45: 989–992, 1995.

Giannicola G. The effects of levodopa and ongoing deep brain stimulation on subthalamic beta oscillations in Parkinson's disease. *Exp Neurol* 226: 120–127, 2010.

Goldman SM. Environmental Toxins and Parkinson's Disease. *Annu Rev Pharmacol Toxicol* 54: 141–164, 2014.

Gradinaru V, Mogri M, Thompson KR, Henderson JM, Deisseroth K. Optical deconstruction of parkinsonian neural circuitry. *Science* 324: 354–359, 2009.

Gross J, Kujala J, Salmelin R, Schnitzler A. Noninvasive Functional Tomographic Connectivity Analysis with Magnetoencephalography. In: Hansen P, Kringelbach M, Salmelin R. *MEG: An Introduction to Methods*. Oxford University Press, 2010 p. 216–244.

Gross J, Tass PA, Salenius S, Hari R, Freund H-J, Schnitzler A. Cortico-muscular synchronization during isometric muscle contraction in humans as revealed by magnetoencephalography. *J Physiol* 527: 623–631, 2000.

Grosse P, Cassidy MJ, Brown P. EEG–EMG, MEG–EMG and EMG–EMG frequency analysis: physiological principles and clinical applications. *Clin Neurophysiol* 113: 1523–1531, 2002.

Hari R. On brain's magnetic responses to sensory stimuli. *J Clin Neurophysiol Off Publ Am Electroencephalogr Soc* 8: 157–169, 1991.

Hari R, Forss N. Magnetoencephalography in the study of human somatosensory cortical processing. *Philos Trans R Soc B Biol Sci* 354: 1145–1154, 1999.

Hari R, Parkkonen L, Nangini C. The brain in time: insights from neuromagnetic recordings. *Ann N Y Acad Sci* 1191: 89–109, 2010.

Hari R, Salenius S. Rhythmical corticomotor communication. *Neuroreport* 10: R1–10, 1999.

Hari R, Salmelin R, Mäkelä JP, Salenius S, Helle M. Magnetoencephalographic cortical rhythms. *Int J Psychophysiol* 26: 51–62, 1997.

Hariz MI, Blomstedt P, Zrinzo L. Deep brain stimulation between 1947 and 1987: the untold story. *Neurosurg Focus* 29: E1, 2010.

Hely MA, Morris JGL, Traficante R, Reid WGJ, O'Sullivan DJ, Williamson PM. The Sydney multicentre study of Parkinson's disease: progression and mortality at 10 years. *J Neurol Neurosurg Psychiatry* 67: 300–307, 1999.

De Hemptinne C, Swann NC, Ostrem JL, Ryapolova-Webb ES, San Luciano M, Galifianakis NB, Starr PA. Therapeutic deep brain stimulation reduces cortical phase-amplitude coupling in Parkinson's disease. *Nat Neurosci* 18: 779–786, 2015.

Hirschmann J, Özkurt TE, Butz M, Homburger M, Elben S, Hartmann CJ, Vesper J, Wojtecki L, Schnitzler A. Distinct oscillatory STN-cortical loops revealed by simultaneous MEG and local field potential recordings in patients with Parkinson's disease. *NeuroImage* 55: 1159–1168, 2011.

Hirschmann J, Özkurt TE, Butz M, Homburger M, Elben S, Hartmann CJ, Vesper J, Wojtecki L, Schnitzler A. Differential modulation of STN-cortical and cortico-muscular coherence by movement and levodopa in Parkinson's disease. *NeuroImage* 68: 203–213, 2013.

Hobson P, Meara J, Ishihara-Paul L. The estimated life expectancy in a community cohort of Parkinson's disease patients with and without dementia, compared with the UK population. *J Neurol Neurosurg Psychiatry* 81: 1093–1098, 2010.

Holsheimer J, Demeulemeester H, Nuttin B, De Sutter P. Identification of the target neuronal elements in electrical deep brain stimulation. *Eur J Neurosci* 12: 4573–4577, 2000.

Hämäläinen M, Hari R, Ilmoniemi RJ, Knuutila J, Lounasmaa OV. Magnetoencephalography–theory, instrumentation, and applications to noninvasive studies of the working human brain. *Rev Mod Phys* 65: 413–497, 1993.

Insola A, Rossi S, Mazzone P, Pasqualetti P. Parallel processing of sensory inputs: an evoked potentials study in Parkinsonian patients implanted with thalamic stimulators. *Clin Neurophysiol* 110: 146–151, 1999.

Jech R, Mueller K, Urgošík D, Sieger T, Holiga Š, Růžička F, Dušek P, Havránková P, Vymazal J, Růžička E. The subthalamic microlesion story in Parkinson's disease: electrode insertion-related motor improvement with relative cortico-subcortical hypoactivation in fMRI. *PloS One* 7: e49056, 2012.

Jensen O, Vanni S. A New Method to Identify Multiple Sources of Oscillatory Activity from Magnetoencephalographic Data. *NeuroImage* 15: 568–574, 2002.

Johnson AN, Wheaton LA, Shinohara M. Attenuation of corticomuscular coherence with additional motor or non-motor task. *Clin Neurophysiol* 122: 356–363, 2011.

Kaasinen V, Vahlberg T, Suominen S. Increasing age-adjusted male-to-female incidence ratio of Parkinson's disease. *Mov Disord* 30: 286–288, 2015.

Kilner JM, Baker SN, Salenius S, Hari R, Lemon RN. Human Cortical Muscle Coherence Is Directly Related to Specific Motor Parameters. *J Neurosci* 20: 8838–8845, 2000.

Kleiner-Fisman G, Herzog J, Fisman DN, Tamma F, Lyons KE, Pahwa R, Lang AE, Deuschl G. Subthalamic nucleus deep brain stimulation: summary and meta-analysis of outcomes. *Mov Disord Off J Mov Disord Soc* 21 Suppl 14: S290–304, 2006.

Krack P, Batir A, Van Blercom N, Chabardes S, Fraix V, Ardouin C, Koudsie A, Limousin PD, Benazzouz A, LeBas JF, Benabid A-L, Pollak P. Five-Year Follow-up of Bilateral Stimulation of the Subthalamic Nucleus in Advanced Parkinson's Disease. *N Engl J Med* 349: 1925–1934, 2003.

Krause V, Wach C, Südmeyer M, Ferrea S, Schnitzler A, Pollok B. Cortico-muscular coupling and motor performance are modulated by 20 Hz transcranial alternating current stimulation (tACS) in Parkinson's disease. *Front Hum Neurosci* 7, 2014.

Kringelbach ML, Jenkinson N, Owen SLF, Aziz TZ. Translational principles of deep brain stimulation. *Nat Rev Neurosci* 8: 623–635, 2007.

Kristeva-Feige R, Fritsch C, Timmer J, Lücking C-H. Effects of attention and precision of exerted force on beta range EEG-EMG synchronization during a maintained motor contraction task. *Clin Neurophysiol* 113: 124–131, 2002.

Kristeva R, Patino L, Omlor W. Beta-range cortical motor spectral power and corticomuscular coherence as a mechanism for effective corticospinal interaction during steady-state motor output. *NeuroImage* 36: 785–792, 2007.

Kühn AA, Kupsch A, Schneider G-H, Brown P. Reduction in subthalamic 8-35 Hz oscillatory activity correlates with clinical improvement in Parkinson's disease. *Eur J Neurosci* 23: 1956–1960, 2006.

Kühn AA, Williams D, Kupsch A, Limousin P, Hariz M, Schneider G-H, Yarrow K, Brown P. Event- related beta desynchronization in human subthalamic nucleus correlates with motor performance. *Brain* 127: 735–746, 2004.

Kuopio A-M, Marttila RJ, Helenius H, Rinne UK. Changing epidemiology of Parkinson's disease in southwestern Finland. *Neurology* 52: 302–302, 1999.

Laitinen L. Surgical treatment, past and present, in Parkinson's disease. *Acta Neurol Scand Suppl* 51: 43–58, 1972.

De Lau LM, Breteler MM. Epidemiology of Parkinson's disease. *Lancet Neurol* 5: 525–535, 2006.

De Lau LML, Verbaan D, Marinus J, van Hilten JJ. Survival in Parkinson's disease. Relation with motor and non-motor features. *Parkinsonism Relat Disord* 20: 613–616, 2014.

Laxton AW, Tang-Wai DF, McAndrews MP, Zumsteg D, Wennberg R, Keren R, Wherrett J, Naglie G, Hamani C, Smith GS, Lozano AM. A phase I trial of deep brain stimulation of memory circuits in Alzheimer's disease. *Ann Neurol* 68: 521–534, 2010.

De Letter M, Aerts A, Van Borsel J, Vanhoutte S, De Taeye L, Raedt R, van Mierlo P, Boon P, Van Roost D, Santens P. Electrophysiological registration of phonological perception in the subthalamic nucleus of patients with Parkinson's Disease. *Brain Lang* 138: 19–26, 2014.

Levy RM, Lamb S, Adams JE. Treatment of chronic pain by deep brain stimulation: long term follow-up and review of the literature. *Neurosurgery* 21: 885–893, 1987.

Li Q, Ke Y, Chan DCW, Qian Z-M, Yung KKL, Ko H, Arbuthnott GW, Yung W-H. Therapeutic Deep Brain Stimulation in Parkinsonian Rats Directly Influences Motor Cortex. *Neuron* 76: 1030–1041, 2012.

Lim M, Kim JS, Chung CK. Oscillatory interaction between the hand area of human primary motor cortex and finger muscles during steady-state isometric contraction. *Clin Neurophysiol Off J Int Fed Clin Neurophysiol* 122: 2246–2253, 2011.

Limousin P, Pollak P, Benazzouz A, Hoffmann D, Le Bas J-F, Perret JE, Benabid A-L, Broussolle E. Effect on parkinsonian signs and symptoms of bilateral subthalamic nucleus stimulation. *The Lancet* 345: 91–95, 1995.

Little S, Pogosyan A, Neal S, Zavala B, Zrinzo L, Hariz M, Foltynie T, Limousin P, Ashkan K, FitzGerald J, Green AL, Aziz TZ, Brown P. Adaptive deep brain stimulation in advanced Parkinson disease. *Ann Neurol* 74: 449–457, 2013.

Litvak V, Eusebio A, Jha A, Oostenveld R, Barnes G, Foltynie T, Limousin P, Zrinzo L, Hariz MI, Friston K, Brown P. Movement-related changes in local and long-range synchronization in Parkinson's disease revealed by simultaneous magnetoencephalography and intracranial recordings. *J Neurosci Off J Soc Neurosci* 32: 10541–10553, 2012.

Litvak V, Eusebio A, Jha A, Oostenveld R, Barnes GR, Penny WD, Zrinzo L, Hariz MI, Limousin P, Friston KJ, Brown P. Optimized beamforming for simultaneous MEG and intracranial local field potential recordings in deep brain stimulation patients. *NeuroImage* 50: 1578–1588, 2010.

Litvak V, Jha A, Eusebio A, Oostenveld R, Foltynie T, Limousin P, Zrinzo L, Hariz MI, Friston K, Brown P. Resting oscillatory cortico-subthalamic connectivity in patients with Parkinson's disease. *Brain J Neurol* 134: 359–374, 2011.

Lopes da Silva FH. Electrophysiological Basis of MEG Signals. In: Hansen P, Kringelbach M, Salmelin R. *MEG: An Introduction to Methods*. Oxford University Press, 2010 p.1–23.

Macleod AD, Taylor KSM, Counsell CE. Mortality in Parkinson's disease: A systematic review and meta-analysis. *Mov Disord* 29: 1615–1622, 2014.

Mamikonyan E, Siderowf AD, Duda JE, Potenza MN, Horn S, Stern MB, Weintraub D. Long-Term Follow-Up of Impulse Control Disorders in Parkinson's Disease. *Mov Disord Off J Mov Disord Soc* 23: 75–80, 2008.

Marsden JF, Limousin-Dowsey P, Ashby P, Pollak P, Brown P. Subthalamic nucleus, sensorimotor cortex and muscle interrelationships in Parkinson's disease. *Brain* 124: 378–388, 2001.

Marttila RJ, Rinne UK, Marttila RJ. Progression and survival in Parkinson's disease. *Acta Neurol Scand* 84: 24–28, 1991.

Mauguière F, Merlet I, Forss N, Vanni S, Jousmäki V, Adeleine P, Hari R. Activation of a distributed somatosensory cortical network in the human brain: a dipole modelling study of magnetic fields evoked by median nerve stimulation. Part II: Effects of stimulus rate, attention and stimulus detection. *Electroencephalogr Clin Neurophysiol* 104: 290–295, 1997.

McClelland VM, Cvetkovic Z, Mills KR. Rectification of the EMG is an unnecessary and inappropriate step in the calculation of Corticomuscular coherence. *J Neurosci Methods* 205: 190–201, 2012.

McIntyre CC, Grill WM. Excitation of central nervous system neurons by nonuniform electric fields. *Biophys J* 76: 878–888, 1999.

McIntyre CC, Savasta M, Kerkerian-Le Goff L, Vitek JL. Uncovering the mechanism(s) of action of deep brain stimulation: activation, inhibition, or both. *Clin Neurophysiol* 115: 1239–1248, 2004.

Medvedovsky M, Taulu S, Bikmullina R, Ahonen A, Paetau R. Fine tuning the correlation limit of spatio-temporal signal space separation for magnetoencephalography. *J Neurosci Methods* 177: 203–211, 2009.

Mendez-Balbuena I, Huethe F, Schulte-Mönting J, Leonhart R, Manjarrez E, Kristeva R. Corticomuscular coherence reflects interindividual differences in the state of the corticomuscular network during low-level static and dynamic forces. *Cereb Cortex N Y N 1991* 22: 628–638, 2012.

Miocinovic S, Somayajula S, Chitnis S, Vitek JL. History, Applications, and Mechanisms of Deep Brain Stimulation. *JAMA Neurol* 70: 163–71, 2013.

Montgomery Jr EB, Gale JT. Mechanisms of action of deep brain stimulation (DBS). *Neurosci Biobehav Rev* 32: 388–407, 2008.

Moreau C, Defebvre L, Destée A, Bleuse S, Clement F, Blatt JL, Krystkowiak P, Devos D. STN-DBS frequency effects on freezing of gait in advanced Parkinson disease. *Neurology* 71: 80–84, 2008.

Myers LJ, Lowery M, O'Malley M, Vaughan CL, Heneghan C, St Clair Gibson A, Harley YXR, Sreenivasan R. Rectification and non-linear pre-processing of EMG signals for cortico-muscular analysis. *J Neurosci Methods* 124: 157–165, 2003.

Mäkelä JP. Bioelectric Measurements: Magnetoencephalography. In: Brahme A. *Comprehensive Biomedical Physics*. Elsevier, Amsterdam, 2014 p. 47–72.

Mäkelä J, Hari R. Long-latency auditory evoked magnetic fields. *Adv Neurol* 54: 177–191, 1990.

Mäkelä JP, Hari R, Karhu J, Salmelin R, Teräväinen H. Suppression of magnetic μ rhythm during parkinsonian tremor. *Brain Res* 617: 189–193, 1993.

Nambu A, Tokuno H, Takada M. Functional significance of the cortico-subthalamo-pallidal "hyperdirect" pathway. *Neurosci Res* 43: 111–117, 2002.

Naskar S, Sood SK, Goyal V. Effect of acute deep brain stimulation of the subthalamic nucleus on auditory event-related potentials in Parkinson's disease. *Parkinsonism Relat Disord* 16: 256–260, 2010.

Neto OP, Christou EA. Rectification of the EMG signal impairs the identification of oscillatory input to the muscle. *J Neurophysiol* 103: 1093–1103, 2010.

Olanow CW, Brundin P. Parkinson's Disease and Alpha Synuclein: Is Parkinson's Disease a Prion-Like Disorder? *Mov Disord* 28: 31–40, 2013.

Olanow CW, Kieburtz K, Odin P, Espay AJ, Standaert DG, Fernandez HH, Vanagunas A, Othman AA, Widnell KL, Robieson WZ, Pritchett Y, Chatamra K, Benesh J, Lenz RA, Antonini A, LCIG Horizon Study Group. Continuous intrajejunal infusion of levodopa-carbidopa intestinal gel for patients with advanced Parkinson's disease: a randomised, controlled, double-blind, double-dummy study. *Lancet Neurol* 13: 141–149, 2014.

Oosterveld LP, Allen Jr. JC, Reinoso G, Seah S-H, Tay K-Y, Au W-L, Tan LCS. Prognostic factors for early mortality in Parkinson's disease. *Parkinsonism Relat Disord* 21: 226–230, 2015.

Østergaard K, Sunde N, Dupont E. Effects of bilateral stimulation of the subthalamic nucleus in patients with severe Parkinson's disease and motor fluctuations. *Mov Disord Off J Mov Disord Soc* 17: 693–700, 2002.

Park H, Kim JS, Paek SH, Jeon BS, Lee JY, Chung CK. Cortico-muscular coherence increases with tremor improvement after deep brain stimulation in Parkinson's disease: *NeuroReport* 20: 1444–1449, 2009.

Pekkonen E, Ahveninen J, Virtanen J, Teräväinen H. Parkinson's disease selectively impairs preattentive auditory processing: an MEG study. *Neuroreport* 9: 2949–2952, 1998.

Perez-Lloret S. Prevalence and Pharmacological Factors Associated With Impulse-Control Disorder Symptoms in Patients With Parkinson Disease. *Clin Neuropharmacol* 35: 261–265, 2012.

Pierantozzi M, Mazzone P, Bassi A, Rossini PM, Peppe A, Altibrandi MG, Stefani A, Bernardi G, Stanzione P. The effect of deep brain stimulation on the frontal N30 component of somatosensory evoked

potentials in advanced Parkinson's disease patients. *Clin Neurophysiol Off J Int Fed Clin Neurophysiol* 110: 1700–1707, 1999.

Piitulainen H, Bourguignon M, De Tiège X, Hari R, Jousmäki V. Coherence between magnetoencephalography and hand-action-related acceleration, force, pressure, and electromyogram. *NeuroImage* 72: 83–90, 2013a.

Piitulainen H, Bourguignon M, De Tiège X, Hari R, Jousmäki V. Corticokinematic coherence during active and passive finger movements. *Neuroscience* 238: 361–370, 2013b.

Poewe WH, Rascol O, Quinn N, Tolosa E, Oertel WH, Martignoni E, Rupp M, Boroojerdi B, SP 515 Investigators. Efficacy of pramipexole and transdermal rotigotine in advanced Parkinson's disease: a double-blind, double-dummy, randomised controlled trial. *Lancet Neurol* 6: 513–520, 2007.

Pogosyan A, Gaynor LD, Eusebio A, Brown P. Boosting Cortical Activity at Beta-Band Frequencies Slows Movement in Humans. *Curr Biol* 19: 1637–1641, 2009.

Pohja M, Salenius S, Hari R. Reproducibility of cortex–muscle coherence. *NeuroImage* 26: 764–770, 2005.

Pollok B, Gross J, Dirks M, Timmermann L, Schnitzler A. The cerebral oscillatory network of voluntary tremor. *J Physiol* 554: 871–878, 2004.

Pollok B, Krause V, Martsch W, Wach C, Schnitzler A, Südmeyer M. Motor-cortical oscillations in early stages of Parkinson's disease. *J Physiol* 590: 3203–3212, 2012.

Pringsheim T, Jette N, Frolkis A, Steeves TDL. The prevalence of Parkinson's disease: A systematic review and meta-analysis. *Mov Disord* 29: 1583–1590, 2014.

Priori A, Cinnante C, Genitrini S, Pesenti A, Tortora G, Bencini C, Barelli MV, Buonamici V, Carella F, Girotti F, Soliveri P, Magrini F, Morganti A, Albanese A, Broggi S, Scarlato G, Barbieri S. Non-motor effects of deep brain stimulation of the subthalamic nucleus in

Parkinson's disease: preliminary physiological results. *Neurol Sci Off J Ital Neurol Soc Ital Soc Clin Neurophysiol* 22: 85–86, 2001.

Priori A, Foffani G, Pesenti A, Tamma F, Bianchi AM, Pellegrini M, Locatelli M, Moxon KA, Villani RM. Rhythm-specific pharmacological modulation of subthalamic activity in Parkinson's disease. *Exp Neurol* 189: 369–379, 2004.

Puschmann A. Monogenic Parkinson's disease and parkinsonism: clinical phenotypes and frequencies of known mutations. *Parkinsonism Relat Disord* 19: 407–415, 2013.

Rasche D, Rinaldi PC, Young RF, Tronnier VM. Deep brain stimulation for the treatment of various chronic pain syndromes. *Neurosurg Focus* 21: E8, 2006.

Remple MS, Bradenham CH, Kao CC, Charles PD, Neimat JS, Konrad PE. Subthalamic nucleus neuronal firing rate increases with Parkinson's disease progression. *Mov Disord Off J Mov Disord Soc* 26: 1657–1662, 2011.

Rosin B, Slovik M, Mitelman R, Rivlin-Etzion M, Haber SN, Israel Z, Vaadia E, Bergman H. Closed-loop deep brain stimulation is superior in ameliorating parkinsonism. *Neuron* 72: 370–384, 2011.

Rossi L, Marceglia S, Foffani G, Cogiamanian F, Tamma F, Rampini P, Barbieri S, Bracchi F, Priori A. Subthalamic local field potential oscillations during ongoing deep brain stimulation in Parkinson's disease. *Brain Res Bull* 76: 512–521, 2008.

Rossini PM, Babiloni F, Bernardi G, Cecchi L, Johnson PB, Malentacca A, Stanzione P, Urbano A. Abnormalities of short-latency somatosensory evoked potentials in parkinsonian patients. *Electroencephalogr Clin Neurophysiol Potentials Sect* 74: 277–289, 1989.

Salenius S, Avikainen S, Kaakkola S, Hari R, Brown P. Defective cortical drive to muscle in Parkinson's disease and its improvement with levodopa. *Brain* 125: 491–500, 2002.

Salmelin R, Hari R. Spatiotemporal characteristics of sensorimotor neuromagnetic rhythms related to thumb movement. *Neuroscience* 60: 537–550, 1994.

Schiefer TKMD, Matsumoto JYMD, Lee KH. Moving forward: advances in the treatment of movement disorders with deep brain stimulation. *Front Integr Neurosci* 5: 69, 2011.

Schnitzler A, Timmermann L, Gross J. Physiological and pathological oscillatory networks in the human motor system. *J Physiol Paris* 99: 3–7, 2006.

Schuepbach WMM, Rau J, Knudsen K, Volkmann J, Krack P, Timmermann L, Hälbig TD, Hesekamp H, Navarro SM, Meier N, Falk D, Mehdorn M, Paschen S, Maarouf M, Barbe MT, Fink GR, Kupsch A, Gruber D, Schneider G-H, Seigneuret E, Kistner A, Chaynes P, Ory-Magne F, Brefel Courbon C, Vesper J, Schnitzler A, Wojtecki L, Houeto J-L, Bataille B, Maltête D, Damier P, Raoul S, Sixel-Doering F, Hellwig D, Gharabaghi A, Krüger R, Pinsker MO, Amtage F, Régis J-M, Witjas T, Thobois S, Mertens P, Kloss M, Hartmann A, Oertel WH, Post B, Speelman H, Agid Y, Schade-Brittinger C, Deuschl G. Neurostimulation for Parkinson's Disease with Early Motor Complications. *N Engl J Med* 368: 610–622, 2013.

Schulz JB, Falkenburger BH. Neuronal pathology in Parkinson's disease. *Cell Tissue Res* 318: 135–147, 2004.

Seppi K, Weintraub D, Coelho M, Perez-Lloret S, Fox SH, Katzenschlager R, Hametner E-M, Poewe W, Rascol O, Goetz CG, Sampaio C. The Movement Disorder Society Evidence-Based Medicine Review Update: Treatments for the Non-Motor Symptoms of Parkinson's Disease. *Mov Disord Off J Mov Disord Soc* 26: S42–S80, 2011.

Siegfried J, Lippitz B. Bilateral chronic electrostimulation of ventroposterolateral pallidum: a new therapeutic approach for alleviating all parkinsonian symptoms. *Neurosurgery* 35: 1126–1129; discussion 1129–1130, 1994.

Soikkeli R, Partanen J, Soininen H, Pääkkönen A, Riekkinen Sr. P. Slowing of EEG in Parkinson's disease. *Electroencephalogr Clin Neurophysiol* 79: 159–165, 1991.

Spiegel EA, Wycis HT, Marks M, Lee AJ. Stereotaxic Apparatus for Operations on the Human Brain. *Science* 106: 349–350, 1947.

Sturm V, Lenartz D, Koulousakis A, Treuer H, Herholz K, Klein JC, Klosterkötter J. The nucleus accumbens: a target for deep brain stimulation in obsessive-compulsive- and anxiety-disorders. *J Chem Neuroanat* 26: 293–299, 2003.

Taulu S, Kajola M. Presentation of electromagnetic multichannel data: The signal space separation method. *J Appl Phys* 97: 124905, 2005.

Taulu S, Simola J. Spatiotemporal signal space separation method for rejecting nearby interference in MEG measurements. *Phys Med Biol* 51: 1759–1768, 2006.

Taulu S, Simola J, Kajola M. Applications of the Signal Space Separation Method. *IEEE Trans Signal Process* 53: 3359–3372, 2005.

Temperli P, Ghika J, Villemure J-G, Burkhard PR, Bogousslavsky J, Vingerhoets FJG. How do parkinsonian signs return after discontinuation of subthalamic DBS? *Neurology* 60: 78–81, 2003.

Timmermann L, Gross J, Dirks M, Volkmann J, Freund H-J, Schnitzler A. The cerebral oscillatory network of parkinsonian resting tremor. *Brain* 126: 199–212, 2003.

Timmermann L, Wojtecki L, Gross J, Lehrke R, Voges J, Maarouf M, Treuer H, Sturm V, Schnitzler A. Ten-Hertz stimulation of subthalamic nucleus deteriorates motor symptoms in Parkinson's disease. *Mov Disord Off J Mov Disord Soc* 19: 1328–1333, 2004.

Ushiyama J, Takahashi Y, Ushiba J. Muscle dependency of corticomuscular coherence in upper and lower limb muscles and training-related alterations in ballet dancers and weightlifters. *J Appl Physiol Bethesda Md 1985* 109: 1086–1095, 2010.

Uutela K, Hämäläinen M, Somersalo E. Visualization of Magnetoencephalographic Data Using Minimum Current Estimates. *NeuroImage* 10: 173–180, 1999.

Volkmann J, Joliot M, Mogilner A, Ioannides AA, Lado F, Fazzini E, Ribary U, Llinas R. Central motor loop oscillations in parkinsonian

resting tremor revealed magnetoencephalography. *Neurology* 46: 1359–1359, 1996.

Walker HC, Huang H, Gonzalez CL, Bryant JE, Killen J, Knowlton RC, Montgomery EB, Cutter GC, Yildirim A, Guthrie BL, Watts RL. Short latency activation of cortex by clinically effective thalamic brain stimulation for tremor. *Mov Disord* 27: 1404–1412, 2012.

Weaver FM, Follett K, Stern M, Hur K, Harris C, Marks WJ, Rothlind J, Sagher O, Reda D, Moy CS, Pahwa R, Burchiel K, Hogarth P, Lai EC, Duda JE, Holloway K, Samii A, Horn S, Bronstein J, Stoner G, Heemskerk J, Huang GD, CSP 468 Study Group. Bilateral deep brain stimulation vs best medical therapy for patients with advanced Parkinson disease: a randomized controlled trial. *JAMA* 301: 63–73, 2009.

Weiss D, Breit S, Hoppe J, Hauser A-K, Freudenstein D, Krüger R, Sauseng P, Govindan RB, Gerloff C. Subthalamic nucleus stimulation restores the efferent cortical drive to muscle in parallel to functional motor improvement. *Eur J Neurosci* 35: 896–908, 2012.

Whitmer D, de Solages C, Hill B, Yu H, Henderson JM, Bronte-Stewart H. High frequency deep brain stimulation attenuates subthalamic and cortical rhythms in Parkinson's disease. *Front Hum Neurosci* 6, 2012.

Willis AW, Schootman M, Kung N, Evanoff BA, Perlmutter JS, Racette BA. PRedictors of survival in patients with parkinson disease. *Arch Neurol* 69: 601–607, 2012.

Witham CL, Riddle CN, Baker MR, Baker SN. Contributions of descending and ascending pathways to corticomuscular coherence in humans. *J Physiol* 589: 3789–3800, 2011.

Zaidel A, Spivak A, Grieb B, Bergman H, Israel Z. Subthalamic span of β oscillations predicts deep brain stimulation efficacy for patients with Parkinson's disease. *Brain* 133: 2007–2021, 2010.

Zrinzo L, Foltynie T, Limousin P, Hariz MI. Reducing hemorrhagic complications in functional neurosurgery: a large case series and systematic literature review. *J Neurosurg* 116: 84–94, 2012.